NTNU

Norwegian University of
Science and Technology

Load and Response Calculation from Breaking Wave Impacts on Columns of Semisubmersible Platforms

Cyril Anglade

Marine Technology
Submission date: July 2017
Supervisor: Jørgen Amdahl, IMT

Norwegian University of Science and Technology
Department of Marine Technology

Acknowledgment

This thesis is the final work required in order to obtain the degree of *Master of Science* in Marine Technology at the Norwegian University of Science and Technology. The work has been performed during the spring semester of 2017, as a continuity of the Specialization Project written during the fall semester 2016.

First of all, I would like to thank my supervisor Professor Jørgen Amdahl for his guidance throughout this year for both the Specialization Project and the Master's Thesis. His advice and knowledge have been particularly helpful and useful for my work. On a larger note, I would like to thank the whole teaching staff of the Institute of Marine Technology for their good work.

I would also like to express my gratitude to my home institution, Ecole Centrale de Nantes, for giving me the chance to fulfill my double-degree at NTNU, as a matter of fact, this Master's thesis represents also the end of my french curriculum.

I would like to thank my friends and fellow students for making my time studying at NTNU an even more enjoyable experience, my family for their help and support and finally Inka, for being immeasurable supportive and constantly brightening up my days.

> *«La mer, compliquée du vent, est un composé de forces. Un navire est un composé de machines. Les forces sont des machines infinies, les machines des forces limitées. C'est entre ces deux organismes, l'un inépuisable, l'autre intelligent, que s'engage ce combat qu'on appelle la navigation.»* Victor Hugo

Trondheim, July 2017

Cyril Anglade

Abstract

Marine structures are subjected to slamming loads during their operating life. Increasing concerns are raised regarding the calculations of extreme loading caused by breaking waves. Slamming loads are associated with high-velocity impacts, large water pressures and short durations. They are challenging to describe and to design against. Traditional methods describing the phenomenon used by regulatory agencies might give inaccurate results. Further, the access to relevant direct numerical calculation approach is rapidly developing.

This study summarizes the results from slamming impacts on different structures in order to assess the role of hydroelasticity using the coupling between a nonlinear FEM analysis and CFD calculations. The link between hydrodynamic flow and response of the structure is discussed, and comparison with rigid body pressure calculations are included. The effects of hydroelasticity, such as the reduction in pressure and deformation, are presented. The importance of hydroelasticity for impact of this magnitude is crucial and needs to be considered.

Using a FEM model with similar characteristics and structural layout as an actual column of mobile offshore unit, the analysis of the response of the platform's column subjected to an extreme slamming load is also carried out Its response and structural integrity are discussed, along with the uncertainties linked to the description of the breaking wave phenomenon. The structure displays deformations within acceptable range for an extreme loading and the operability and load bearing function of the structure is moreover not directly endangered.

Contents

List of Figures

List of Tables

Abbreviations

ULS	Ultimate Limit State
ALS	Accidental Limit State
c	Wave phase velocity
C_{br}	Breaking crest velocity
CFD	Computational Fluid Dynamics
EI	Bending stiffness
k	Wave number
α	Deadrise angle
ρ	Mass density of water, ρ=1025kg.m^{-3}
σ	Stress, in MPa
ϵ	Strain, in m.m^{-1}
ζ	Wave elevation, in m
λ	Wavelength, in m

Chapter 1

Introduction

Environmental conditions at sea can be very harsh and the marine structures built by humans have to withstand perpetual loads coming from various origins during decades. Wind, current and waves are acting on those structures during their whole service life. Offshore structures are very often remote autonomous constructions and any failure occurring could be disastrous. Many examples throughout the history of the Oil & Gas industry prove the hazards linked to those structures. Structural failures, ship collisions, extreme environmental conditions, defects in the petroleum systems leading to fires or explosions and dropped objects are all threats to the integrity of an offshore platform. As recently as late December 2015, a rig in the Troll field in the North Sea has been hit by a steep wave, leading to one death and several injuries among the crew members and extensive structural damage on the platform. This accident shed light on the lack of regulation and accurate recommended practices concerning the event of a large wave breaking on a platform. The platform in question, COSL Innovator, was in accordance with the requirements defined by DNV GL and the Petroleum Safety Authority (PSA). The investigations following the accident made it clear that the guidelines "have been too vague with regard to the applicable calculation methodology for horizontal wave forces on mobile units", reported the PSA.

The social, environmental and economic risks linked with offshore accidents are high. Marine structures are thoroughly designed and maintained throughout their whole life-cycle. In addition, the *safe life* method is often employed in order to account for uncertainties in the loading,

the material or human errors. It means that certain members can fail without having an accidental impact on the rest of the structure. Most accidental events are challenging to design against and the regulations set are often based on scientific literature. Most of the guidelines are conservative for obvious reasons, but the case of horizontal wave forces on offshore mobile units, i.e. semi-submersibles, seems to lack in precision.

The actual impact that extreme breaking waves can have on semi-submersible platforms needs therefore to be assessed. The usual way of calculating the loads from such events is by using model tests in basins. However, this way of calculating the loading has flaws that will be explained later in this paper. The approach preferred for this thesis is a coupled analysis using the simulated behavior of the flow during the slamming impact of the wave on the structure. CFD analysis, although computationally challenging, is seeing more and more use in order to solve complex fluid-structure interaction. It also allows for more flexibility than model experiments, as several configurations can be simulated for usually in less time and at lower cost than traditional methods. In this thesis however, the full use of CFD will not be made as the results of the simulations will mostly be described and analyzed from a structural point of view; the actual behavior of the flow during and after the impact is not within the scope of the study.

In order to obtain accurate data, the column whose structural integrity will be assessed in this thesis is using slightly modified plans and drawings of an actual semi-submersible platform in use on the Norwegian Continental Shelf.

1.1 Background

Every marine structure is subjected to wave loading, but the influence of wave loading and the magnitude of the forces at stake differs for every type of floating or surface piercing body. Breaking waves impacts have specially to do with high structures and can be damageable both for load bearing members, such as columns and braces and because of problems related to green water, wave-in-deck, etc. There exist several different kinds of marine structures but a recurrent design consists of slender surface-piercing members, particularly conductive to wave impacts. Out of

the designs used for offshore platforms, semi-submersible platforms are especially vulnerable to slamming loads, due to their stabilizing columns offering a large surface area, an example of a floating platform is illustrated in Figure 1.1. The platform stays afloat thanks to two pontoons and several hollow columns providing sufficient buoyancy and stability for safe operability of the platform. The exposure to slamming is therefore inherent to the design.

The material used for the structural members of the platform can differ from one unit to another. Both concrete and structural steel can be used. Concrete structures are particularly durable and resistant to impacts and collisions (Sandvik, 2004), the concern about significant damage caused by slamming is therefore limited. As of today, most of the floating platform are built with structural steel, constituted by welded stiffened panel. Steel displays an elastic behavior and is likely to suffer large deformations and damages in the case of an extreme impact with a breaking wave.

Figure 1.1: Floating platform Visund, located offshore Norway, with its four large stabilizing columns (Photo: http://www.offshoreenergytoday.com)

The real loads induced by breaking waves on the structures are potentially higher than those defined by for example classification companies, such as what is described in Section 8 of the Recommended Practice DNV-RP-C205: Environmental conditions and environmental loads (2010). Two particular design limits are important when it comes to extreme wave loading, namely the Ultimate Limit State (ULS) and the Accidental damage Limit State (ALS). According to NORSOK N-003 (NORSOK, 2007), in order to be safe regarding to the ULS, a structure has to withstand

a combination of environmental loads corresponding to an annual exceedance probability of 10^{-2}. Concerning ALS, the structure shall be able to maintain the prescribed load carrying function for the defined accidental actions, i.e. 10^{-4} annual exceedance probability. The ALS is a way to define the absolute highest load resistance requirement for a structure, and it can give us a basis in order to define the dimensions of the wave that has to be considered for this study.

1.2 Objectives

The wave slamming on offshore structures is a crucial and threatening event for the structural integrity of the constructions. The main goal of the study is to assess whether a column of a floating offshore platform can be able to withstand the loads provoked by a wave corresponding to the ALS conditions breaking exactly on the column. The main steps leading to the resolution of the problem are:

- Defining the parameters of the *design wave* used for the slamming impact
- Simulating the slamming impact on simple models and discussing the role of hydroelasticity in slamming
- Assessing the structural integrity of the column after the event described above using a coupled simulation

1.3 Limitations

The main limitation of this work is the actual modeling of the wave. First of all, the parameters of the ALS wave can only be extrapolated from statistics and and extreme distribution models, this may lead to approximate data which can have an impact on the real life results. Secondly, the wave profile is very hard to describe because of the high nonlinearity of the event, and the shape of the flow is simplified in this paper's approach. Moreover, the *design wave* used in the work is the only environmental loading applied to the structure, while the wind and the current are discarded, all of which can potentially have an impact on the behaviour of the structure during extreme environmental conditions.

1.4 Outline of the Thesis

The background needed in order to comprehend and analyze properly the event in question, such as hydroelasticity or slamming, is presented in Chapter 2. A literature review and calculations needed for this work's analysis are present for each section. Chapter 3 & 4 describe the setup of the simulation carried out, the models and meshing configurations, as well as the setup of the softwares used.

Then, the results from the simulation of slamming events on simple models are presented and discussed in Chapter 5. Stiffened panels are used in order to get first results on the structural response to slamming. Two types of coupling are used for the simulation in this chapter, the aim is to assess the impact of hydroelasticity by using two body stiffnesses in the fluid dynamics problem.

In Chapter 6, the simulation of the slamming of a breaking wave on a platform column and results of its structural integrity are discussed. Finally, the comparison between the global response of the column and the responses from the previous chapter is also done and the results are discussed. Finally, recommendations for further work are given.

Chapter 2

Theory

2.1 Hydroelasticity

Hydroelasticity refers to the interaction between a structure and the fluid it is relatively moving through. A body under water pressure will deform and change of overall geometry, this leads to a reduction of the pressure applied on the body, thus leading to less deformation. It is important to assess whether hydroelasticity is important for slamming events. As presented by Bereznitski (2001), the hydroelasticity has often been questioned for slamming and it is important to note that hydroelasticity can only ever happen if the structure deforms and its effect can be significant (Arai and Miyauchi, 1998). Hence, the basin tests, realized with stiff panels, cannot account for hydroelasticity as the loads applied are not high enough to deform the structure significantly. Thus, the deformation of the structure and its impact on the fluid cannot be accounted for. Moreover, the large pressures happen for small deadrise angles as presented in Section 2.5, which makes hydroelasticity particularly relevant for those impacts. A general criterion often used in literature is that the coupled effects are likely to be significant when the natural period is at least two times the duration of the impact (Bereznitski, 2001). Its importance increases when the impact velocity and the highest natural period of the local structure (Faltinsen, 2000). Faltinsen (1999) established a criterion to determine whether hydroelastic effects

matters for slamming on stiffened plates between bulkheads:

$$\sqrt{\frac{EI}{\rho L^2}}\frac{tan\alpha}{|V_R|} < 0.25 \tag{2.1}$$

Where EI is the bending stiffness of a representative beam, L is the length of the beam, α is the angle of impact and V_R is the relative normal velocity.

As explained by Bereznitski (2001), hydroelasticity leads to a reduction of water pressure during impact and a distribution of the load over a longer time. These effects could reduce structural deformations up to 75%. The action of hydroelasticity is comparable to entrapped air between the structure and the fluid, which can lead to a reduced pressure due to cushioning efffects.

2.2 Plasticity

In the case of strong fluid impact with the structure, large stresses are likely to occur in the structure and can surpass the yield strength of the material. When this happens, the relation between the stress and the strain, which is illustrated by Hooke's law (1678) in the elastic domain ($\sigma = E\epsilon$, where σ, E and ϵ are the stress, Young's modulus and the strain, respectively), becomes nonlinear. Material like structural steel show a strain hardening behavior when plastic deformation occurs, see Figure 2.1. The stress-strain relationship has been studied and described in several ways, the most commonly used being the formula from Ramberg and Osgood (1943).

In Figure 2.1, several points on the curve are of interest. σ_{PL} is the *proportionality limit*, it is the stress over which the strain-stress relationship becomes non-linear. σ_{EL} is the *elasticity limit*, under this stress value no permanent strain will remain on the structure after unloading. σ_{YP} represents the *yield point* which produces a specified value of plastic strain. Finally, σ_U, the *ultimate stress*, is the maximum stress on the strain-stress curve. Plastic strain is of concern when permanent deformations are large because they lead to rupture of shell plating or failure of supporting members (Wang et al., 2002).

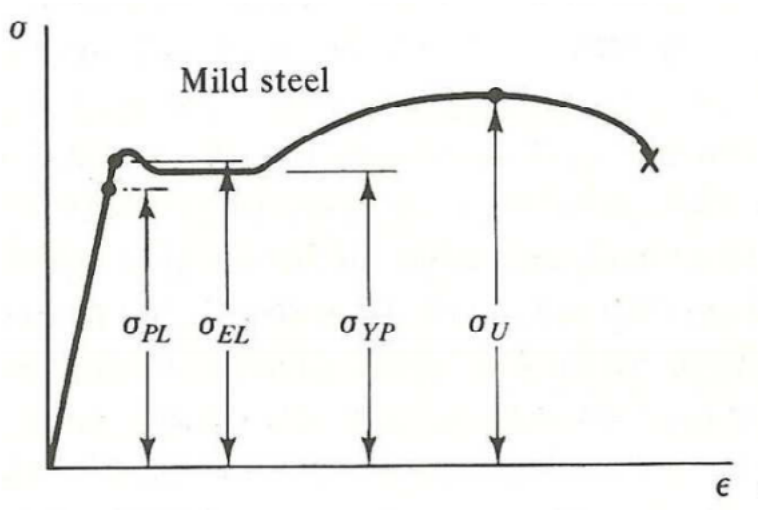

Figure 2.1: Strain-stress curve for a strain hardening material

Elastic-plastic deformation can occur in the structure during the impact with the fluid. Both an elastic wave and a plastic wave propagate simultaneously in the solid medium (Liu et al., 2008). The interaction structure/water when plastic deformation occurs is a topic that still need to be studied thoroughly, and the most accurate method to account for hydro-elasto-plasticity is to perform Fluid-Structure Interaction (FSI) analyses, even though it remains a challenge to obtain similar results between experiments and simulations (Portemont et al., 2004).

2.3 Fluid-Structure Interaction in a Dynamic Problem

"Coupled systems and formulations are those applicable to multiple domains and dependent variables which usually describe different physical phenomena and in which neither domain can be solved while separated from the other and neither set of dependent variables can be explicitly eliminated at the differential equation level" (Zienkiewicz et al., 2005).

Two main methods are used to solve a mechanical problem, static and dynamic analysis. A system is said to be *static* if its behavior is independent of time. Static analyses are used for problems where inertia forces are non-significant. In this study, inertia forces are predominant and are highly time-dependent. A static analysis would therefore give results that are not relevant. On the other hand, dynamic analyses are used for problems where inertia forces are varying in

time. In the case of slamming, the acceleration can reach $100g$ (Engle and Lewis, 2003), proving the need for a dynamic solving of the problem.

In addition to the usual discretization of space in elements for the Finite Element Method, the problem is also discretized time-wise. The dynamic equilibrium equation of the system (Eq. 4) has to be solved for each time step of the problem.

FSI problems combine different physical domains interacting with each other. In the present case, both fluid dynamics and structure dynamics are vital in the solving process. The fluid motions are solved thanks to the Navier-Stokes equation.

$$\frac{\partial \rho}{\partial t} + \frac{\partial (\rho u_i)}{\partial x_i} = 0 \tag{2.2}$$

$$\frac{\partial (\rho u_i)}{\partial t} + \frac{\partial [\rho u_i u_j]}{\partial x_j} = -\frac{\partial p}{\partial x_i} + \frac{\partial \tau_{ij}}{\partial x_j} + \rho f_i \tag{2.3}$$

On the other side, the structural response is calculated by discretizing the structure using a Finite Element Method.

$$M \cdot \ddot{\vec{u}} + C \cdot \dot{\vec{u}} + K \cdot \vec{u} = \vec{F} \tag{2.4}$$

Where M, C, K are the mass, damping and stiffness matrices, respectively, u is the displacement and F represents the loading acting on the system.

Both the fluid domain and the solid domain must be discretized carefully in order to achieve accuracy. When considering the slamming phenomenon on a platform, the deformations caused to the structure can be important. The deformed structure may interact with the fluid differently from the original one. In order to assess the extent of the differences, a Fluid-Structure-Interaction problem can be solved in two different ways, either by a one-way coupling or a two-way coupling. Both processes are described in Figure 2.2. At a definite time step, the solution of

the fluid is computed, the forces acting on the structure are then transmitted to the structural solver and the mechanical solution is calculated. The fluid mesh remains untouched during the process, while the structure is deformed. The two-way coupling uses the deformations and displacements from the structure in order to update the fluid mesh to the actual shape. This means that the two-way coupling uses the process of the one-way coupling multiple times until the displacement and the forces converge before going onto the next time step, see Figure 2.2.

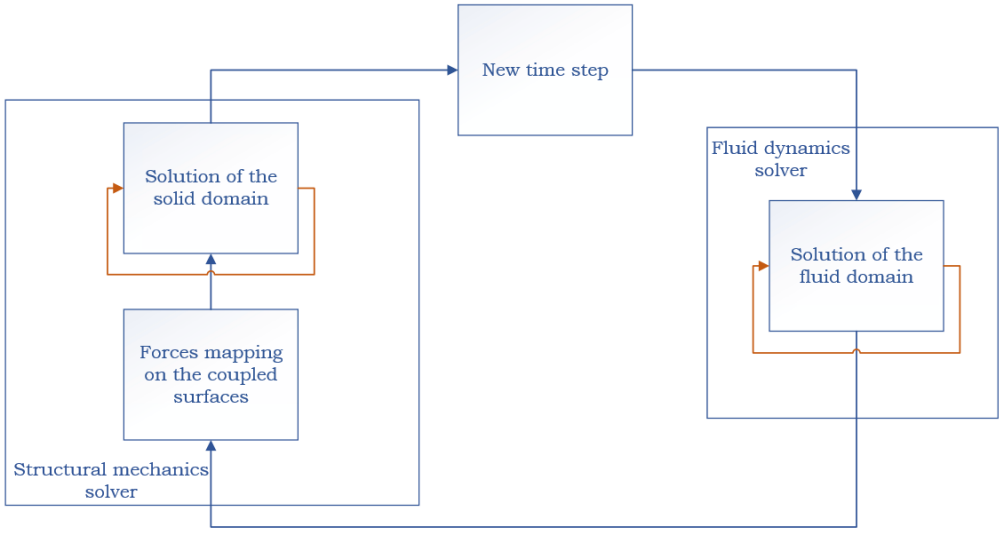

(a) One-way coupling

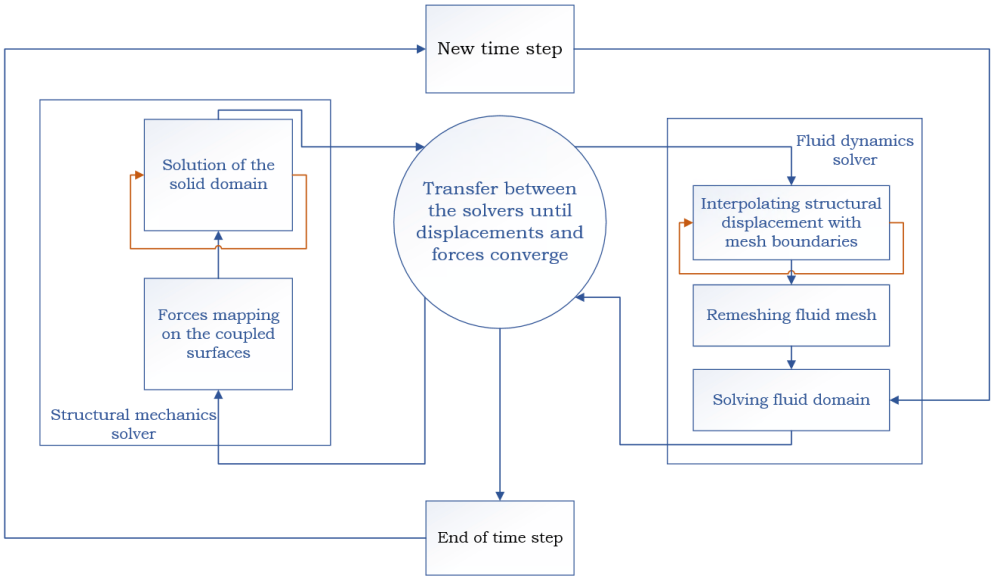

(b) Two-way coupling

Figure 2.2: Representation of the algorithms for the one-way and two-way couplings (Benra et al., 2011)

The difference between both problems is minor for cases leading to small deformations because the deformed fluid mesh has little to no impact on the solution. However, the two-way coupling is required for large deformations problems, but can lead to very high computation times.

2.4 Nonlinear Wave Theory

2.4.1 Breaking Wave Criteria

The phenomenon of waves breaking has been studied for a long time and is still a domain of particular interest. Breaking waves can occur both in shallow and deep water. However, the field of study of the present problem is about offshore structures, therefore the mechanisms of shallow water breaking waves will not be presented here.

Geometric Criteria

A 2D linear wave is easily and fully described by only two parameters, its wave amplitude ζ_a and wavelength λ, see Figure 2.3. Those two numbers lead to the calculation of a fundamental parameter when it comes to breaking waves, the steepness, calculated from:

$$k\zeta_a = \frac{2\pi\zeta_a}{\lambda} \tag{2.5}$$

Where k is the wave number.

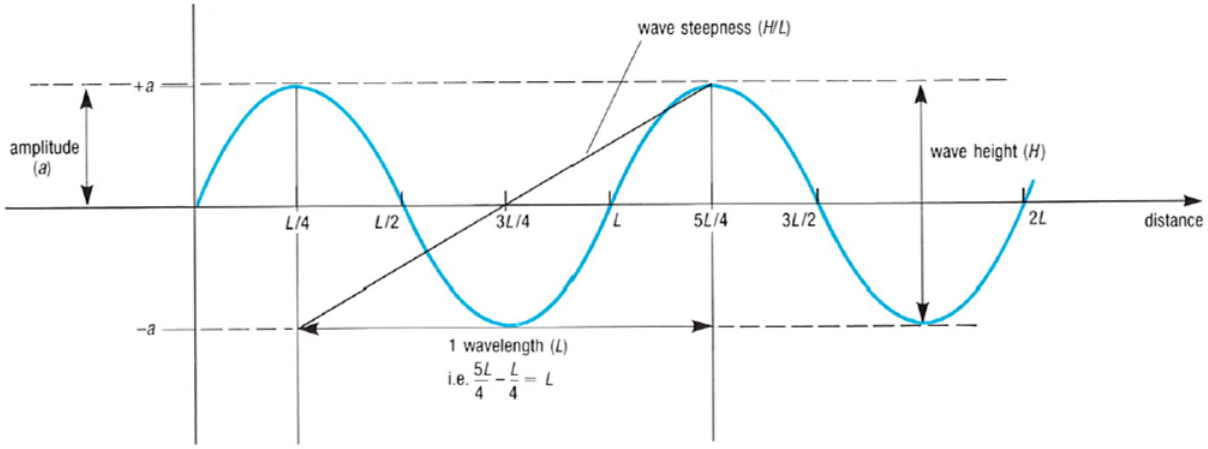

Figure 2.3: Description of the parameters of a linear wave

Under a certain range of steepness, gravity waves are linear, but when the product $k\zeta_a$ increases, the waves tend to become nonlinear and asymmetrical. The theory of Stokes (1880) predicts that a limit is reached for a crest angle of 120° ($k\zeta_a = 0.443$), and wave breaking occurs above this angle, while Duncan (1983) found a limiting steepness as low as 0.31. In practice, wave breaking

is a very unsteady and highly nonlinear phenomenon, dependent on more than the sole steepness. The local wave geometry of a steep wave is very different from a linear wave, the wave gets horizontally asymmetric as the wave-crest steepens and the wave-trough flattens. Moreover, the front of the wave also steepens, as illustrated by Perlin et al. (2013) in Figure 2.4. As a plunging breaker gets closer to its breaking point, the front of the wave becomes almost vertical due to a higher wave particle velocity in the wave crest and forms a moving wall which overturns and collapses down in the water shortly after. Among others, breaking crest asymmetry and energy dissipation rate are other factors that can affect the phenomenon. More parameters were introduced by Kjeldsen and Myrhaug (1979) to describe a nonlinear wave, such as the crest-front steepness ϵ, crest-rear steepness δ and the horizontal and vertical asymmetry (μ and β, respectively).

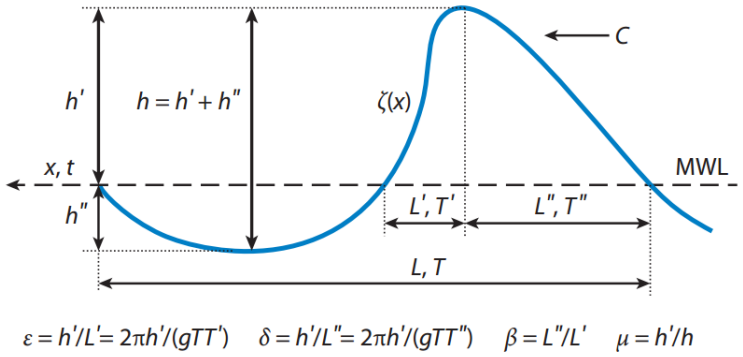

Figure 2.4: Representation of local nonlinear wave geometry

The importance of the parameter ϵ is great with regard to an impact between a breaking wave and a floating structure. Kjeldsen and Myrhaug (1979) reported breaking crest-front as high as 0.78. However, it has been found by Tian et al. (2010) that a wave increases in slope immediately before wave breaking occurs, which might lead to more violent wave breaking.

Kinematic Considerations

The geometry deformation of steep waves implies a difference in water particle velocity between the crest and the rest of the wave. The nonlinear wave will ultimately break when the horizontal crest particle velocity U surpasses the phase velocity c (Tian et al., 2010). For the purposes of the current analysis, the breaking crest speed c_{br} is of major interest, as it will help to determine the

speed of the impact between the wave and the platform. This breaking crest speed c_{br} is reportedly close to the linear wave speed c, with values ranging from $c_{br} = 0.8c$ (Melville and Matusov, 2002) to $c_{br} = 0.9c$ (Banner and Peirson, 2007; Stansell and MacFarlane, 2002). However, it is possible to use these values in order to define more parameters of the "design wave" used for the simulation in this paper. The crest height of the waves corresponding to the ULS and ALS design waves were estimated based on measurements from a particular North Sea location by extrapolating metocean data with the help of Forristall's model, see Table 2.1.

Table 2.1: ULS and ALS values for different parameters in the North Sea from Lian and Haver (2015)

Annual probability of exceedance	Crest height (m)	Significant Wave height (m)	Peak period (s)
10-2	16.8	15.0	16.6
10-4	21.8	18.5	18.5

2.4.2 Definition of the design wave

Using the crest height which has an annual probability of exceedance of 10^{-4}, it is possible to estimate the wave height corresponding to the ULS condition. Bonmarin et al. (1989) measured the horizontal asymmetry parameter of breaking waves, and reported values ranging from 0.6 two hundred milliseconds prior to breaking to 0.7 right before the breaking moment. Using Table 2.1 and 0.7 as a value for μ, we have:

$$h = \frac{h'}{\mu} = \frac{21.8}{0.7} = 31.1m \tag{2.6}$$

Thus, with Stokes' limiting steepness criteria, the wavelength of the equivalent linear design

wave reads:

$$k\zeta_a = 0.44 \tag{2.7}$$

$$\frac{2\pi}{\lambda} = \frac{0.44}{\zeta_a} \tag{2.8}$$

$$\lambda = \frac{28.8 \cdot 2\pi}{0.44} \tag{2.9}$$

$$\lambda = 444m \tag{2.10}$$

According to the linear theory, in deep water, the wave angular frequency $\omega = \frac{2\pi}{T}$ is linked to the wave number k and the acceleration of gravity g by the relation:

$$\omega^2 = gk \tag{2.11}$$

The wave celerity reads:

$$c = \frac{\omega}{k} = \frac{\sqrt{gk}}{k} = \sqrt{\frac{g}{k}} \tag{2.12}$$

Using Eq. 2.5,

$$c = 26.3m.s^{-1} \tag{2.13}$$

These calculations are based on linear wave theory, however, the waves studied are highly non-linear and the phase speed cannot be extrapolated from the equivalent linear waves (Stansell and MacFarlane, 2002). Studies are often using monochromatic waves and small scale experiments, making it difficult to assess the parameters in an actual environment. Moreover, maximal wave height are based on spectra and fitted distribution that can be inaccurate when defining extreme values. A wave with a height corresponding to the ALS condition can result from a superposition of several smaller waves and thus have a phase speed significantly lower than the ones assumed above. As a first approach, a breaking crest speed of $c_{br} = 0.85 \cdot 26.3 \simeq 22m.s^{-1}$ will be used in this paper, but some uncertainties remain when it comes to the calculation of the crest speed.

As a comparison, one can use the recommendations from DNV (2010) for the breaking wave parameters:

> For undisturbed waves, the impact velocity (u) should be taken as 1.2 times the phase velocity of the most probable highest breaking wave in n years. The most probable largest breaking wave height may be taken as 1.4 times the most probable largest significant wave height in n years.

Thus, using Table 2.1, the most probable largest breaking wave height in 10000 years is

$$H = 1.4 \cdot 18.5 = 25.9m \tag{2.14}$$

Which, with the same reasoning as before, leads to an impact velocity $u = 24m.s^{-1}$. This result confirms the calculation above.

The exact angle of impact of the breaking wave on the structure is a challenging topic. Experiments show that the overturning moment is very sudden and the fluid direction changes constantly during the breaking event, which leads to a difficult assessment of the angle between the fluid and the structure. As presented in the next section, the configuration leading to the most violent impact is with a vertical crest-front and a horizontal direction, which is the one used in this thesis.

2.5 Slamming

Slamming defines the water impact loads on a structure, it is relevant both locally due to the high pressure induced, and globally, by a phenomenon also known as whipping. It is characterized by large hydrodynamics loads and a short duration, making it an important phenomenon to design against which has to be investigated carefully. Most marines structures are subjected to slamming, from hulls of ships to internal tanks filled with liquid and offshore platforms. Several assumptions are made in the model used in this paper in order to simplify the calculations when it comes to slamming. The fluid, which in the current case is water, is assumed to be incompressible and inviscid and the flow is assumed to be irrotational. Moreover, due to the very high fluid acceleration compared to the acceleration of gravity, the effects of gravity are disregarded for the experiments. It has been shown that compressibility of water can actually matters in some cases (Campana et al., 2000). A constant velocity is also assumed, the usual way of describing slamming is using a still flat fluid and a falling body, however in this paper, the body is almost immobile while the water is assumed to have a constant velocity during the short moment of impact.

The theory of the impact force of the slamming event has been a field of concern ever since it was first described by von Karman (1929) and then generalized by Wagner (1932). Von Karman's theory of impact for a 2D rigid wedge uses a still waterline during the water entry, while Wagner's theory accounts for run-ups along the body, leading to a higher wetted surface, as illustrated in Figure 2.5. The first studies focused mainly on wedges, which have the particularity of having a constant deadrise angle during water entry. More difficulties for the study of the slamming phenomenon for a deadrise close to or equal to zero. A null deadrise angle leads to a numerical singularity, calling for different methods of resolution.

Remark: The deadrise angle is the angle between the still water line and the tangent line drawn at the surface of the body at the point where the water suface and the body are intersecting.
The solution of the problem for circular bodies has been studied later, particular with by Faltinsen and Zhao (1993) and Zhao et al. (1996) using the boundary element method (BEM) ap-

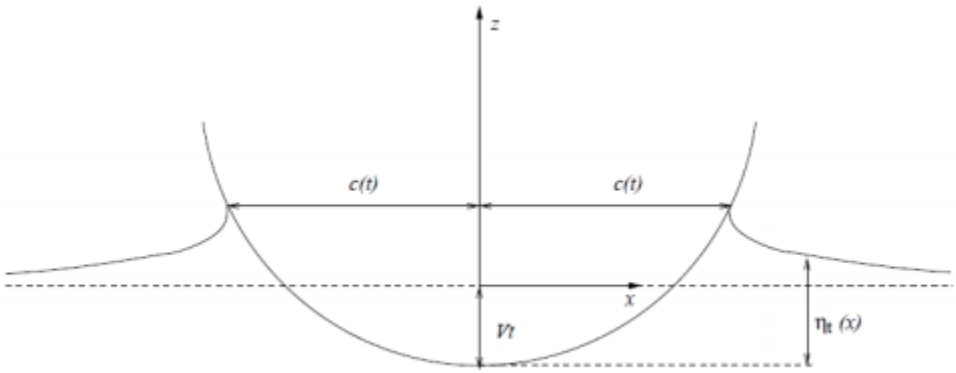

Figure 2.5: Water entry of a circular cylinder according to Wagner's theory

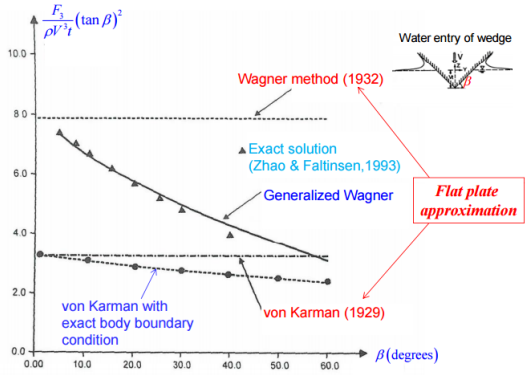

Figure 2.6: Comparison of slamming forces for different theories

proach to solve the problem in two dimensions, generalized later for three-dimensional bodies by Faltinsen and Chezhian (2005). The comparison of the slamming forces expected with several theories is illustrated in Figure 2.6. It can be seen that von Karman's theory clearly underpredicts the water entry force, whereas Wagner's theory overestimates it.

The comparison of slamming forces is often done through a slamming coefficient C_p defined by:

$$C_p = \frac{P_{max} - P_0}{\frac{1}{2}\rho V^2} \tag{2.15}$$

Where P_{max} is the maximum pressure, P_0 the reference pressure and V the water entry velocity. It is important to note that the high pressure peak associated with slamming is not necessarily the most important parameter for the estimation of the structural response (DNV, 2010). Space-

averaged slamming pressure is particulary relevant. It is calculated from:

$$p_s = \frac{1}{2}\rho C_{pa} v^2 \tag{2.16}$$

Where p_s is the space average pressure, ρ the mass density of the fluid, C_{pa} the space average slamming coefficient and v the relative normal velocity between the fluid and the surface of the body.

The duration of the impact is also relevant for the setup of the analysis. It may be taken for a vertical cylinder as:

$$T = \frac{13D}{64c} \tag{2.17}$$

Where D is the diameter of the cylinder and c is the phase velocity (Wienke et al., 2004). With the calculated phase velocity in Eq. 2.13 and the diameter of the column studied, it becomes:

$$T = 0.094s \tag{2.18}$$

The shock pressure resulting from the impact is thus very short. Once the shock pressure and the hydroelastic phase is over, the dynamic pressure decreases quickly and the main pressure component on the cylinder is the usual force of a wave deriving from the Morison equation (Morison et al., 1950):

$$F = \int_{-d}^{\eta} \frac{1}{2}\rho C_D D \cdot u(z)|u(z)|dz + \int_{-d}^{\eta} \rho C_M \frac{\pi D^2}{4} \cdot \dot{u}(z)dz \tag{2.19}$$

Where ρ: water density, D: cylinder diameter, η: water surface elevation, d: water depth, C_M and C_D are forces coefficients determined experimentally, but known for common geometries.

The force from Morison equation can also be used in design in order to calculate the impact force of breaking waves as (Wienke and Oumeraci, 2005):

$$F_{br} = 2.5F \tag{2.20}$$

This formula gives a theoretical value to design against, however, it does not give any relevant information about the loading history over time.

Model experiments are wildly use in order to verify theories, and the setup often used is a drop test of bodies in water, with either rigid or elastic bodies. The validity of results from drop-test experiments remains for different configuration, such as the impact of a wave on a vertical cylinder. This is because gravity does not matter, making the direction of the impact unimportant.

2.6 Global relevance of slamming

So far, only local effects have been considered. It is important to consider the effect of extreme waves on a global scale and assess whether they can have an impact on the overall stability of the structure. A high wave can be enough to capsize a small vessel, due to the angular momentum in roll direction transferred from the wave (Nedrelid, 1983). However, Huse and Nedrelid (1985) studied the effect of waves in the capsizing process of a semi-submersible and the direct result is that extreme breaking waves cannot make the structure capsize. The main difference between the semi submersible and a small ship is the metacentric height in roll, making the righting moment a lot higher for a semi-submersible. However, large wave heights can have an impact on the heeling angle of the platform (Voogt et al., 2002), which can affect operability.

Moreover, in the case of an extremely large wave, the air-gap, i.e. the difference in elevation between the bottom of the deck and the mean water level, might be too small and lead to a negative instantaneous air-gap, meaning that the deck can be momentarily under the water surface. This causes both vertical and horizontal wave-in-deck forces due to the wave hitting the bottom and the side of the deck, respectively. This issue is also crucial for the offshore industry, but is not within the scope of the study. Abdussamie et al. (2014) carried out extensive simulations on this topic.

Chapter 3

Analysis Setup

This chapter introduces the methods used for the simulation work. The softwares used and their configurations will be presented.

3.1 Softwares Configuration

The main component is the software ANSYS Workbench 17.2. First of all, the geometry of the column is designed through ANSYS DesignModeler 17.2. For the structural part of the analysis, the geometry is meshed and transformed into a Finite Element Model in ANSYS Mechanical. On the other hand, the fluid dynamics problem only requires the outer shell of the column for its analysis. The model is therefore composed of a fluid domain with a simple cylinder with the column's dimensions in the center. The fluid dynamics analysis is carried out thanks to ANSYS Fluent 17.2, while the structural analysis is achieved with the « Transient Structural » component of ANSYS Mechanical. Both softwares are ran simultaneously and the data transfer between them is assured by a System Coupling.

The technique used for the CFD solver is the Volume of Fluid (VOF) method. It is widely used to simulate complex free surface deformation as it allows for break-up of particles a large changing in the topology of fluid domain (Kleefsman et al., 2004). Each cell of the fluid domain is given a volume fraction f for each fluid (Marcer et al., 2010). In a two fluid system:

- $f = 1$ signifies that the cell is filled with water

- $f = 0$ signifies that the cell does not contain any water, and is thus filled with air
- $0 < f < 1$ signifies that the cell contains an interface air-water.

As seen previously, drop tests are a common way to study the slamming phenomenon, but the neglectable effect of gravity leaves the possibility to simulate the event in any direction. Simulating a drop test in a CFD software requires both a high computation time and a high CPU usage. As a matter of fact, moving an object through the fluid mesh at a high velocity requires the remeshing of the fluid domain at each time step, which slows the process and can lead to skewed elements. This is why the chosen solution to carry out the simulation is using an immobile structure with a moving fluid, see Figure 3.1a. An additional advantage of using an immobile structure is the possibility to simulate the short impact of the wave on the structure. Given that, the amount of water impacting the column is not infinite, and the impacted area of the column is in air a short while after being hit by the wave. Then, it is possible to modify the type of boundary conditions of the fluid domain in order to stop the flow after a certain time by modifying the *inlet* boundary to a *wall*, see Figure 3.1b. The other boundaries are of the type *outflow*, allowing the fluid to flow freely out of the fluid domain. This type of boundary is chosen over *wall* in order to avoid the reverse flow of the fluid when it hits a wall, which could disturb the results of the simulation.

The velocity and the direction of the fluid going through the inlet are controlled and setup with the parameters corresponding to the highest breaking wave in a 10,000 years period. The direction of the fluid is therefore normal to the column's axis, and the fluid velocity is $u = 22m.s^{-1}$. This leads to an idealized event, with all particles having the same directions and velocity.

For the one-way coupling, the boundaries of the panel are extracted and used as rigid walls by the fluid solver. This mode of simulation is similar to using model tests in order to acquire a loading history of the wave on the model and apply the resulting forces in the mechanical solver. However, the two-way coupling uses the actual shape of the structure as a boundary in the fluid solver.

The flow behind the cylinder is not within the scope of the study, as only the impact and a short while after it is to be considered in the slamming event. Thus, only a quarter of the cylinder is represented, and the fluid domain is restricted to a small volume around the cylinder for better accuracy and shorter computation time.

The fluid solver is using a transient simulation and a pressure-based solver in order to simulate accurately the impact of the fluid on the structure. The pressure-based solver is using a pressure equation and is mostly used for incompressible flows. The fluid used is water, with a mass density $\rho = 1025 kg.m^{-3}$. The turbulence model used is the $k-\omega$ model with default properties.

3.2 Convergence issues

The configuration for the simulation of a shock event is a challenging task when attempting convergence during the computation. The time stepping must be appropriate and small enough to catch the rapid variation in loading and update the fluid and structural domains. For CFD calculations, the maximum allowable time step is dependent on the mesh size (Larsen, 2013). The maximum Courant–Friedrichs–Lewy (CFL) number allowed in this thesis is 5 over the whole domain. When it comes to the structural solver, the high shock pressure from slamming requires to be divided in a large number of time steps to achieve convergence. A large time step leads to convergence difficulties and many bisections in the steps make the calculations longer than they should be. On the other hand, if the time stepping is too refined, the calculations can also become unnecessarily long. In this thesis, a time step of $\Delta t = 0.1 ms$ is used throughout the simulation. Using five coupling iterations per time step, both solvers were able to reach RMS (root mean square) residual values - the main measure of convergence - below $1e^{-4}$ except for the later parts of the main simulation, which is considered as sufficient for most engineering problems (Ajayi et al., 2014). Without performing systematic studies, the under-relaxation factors in Fluent had to be modified for better convergence.

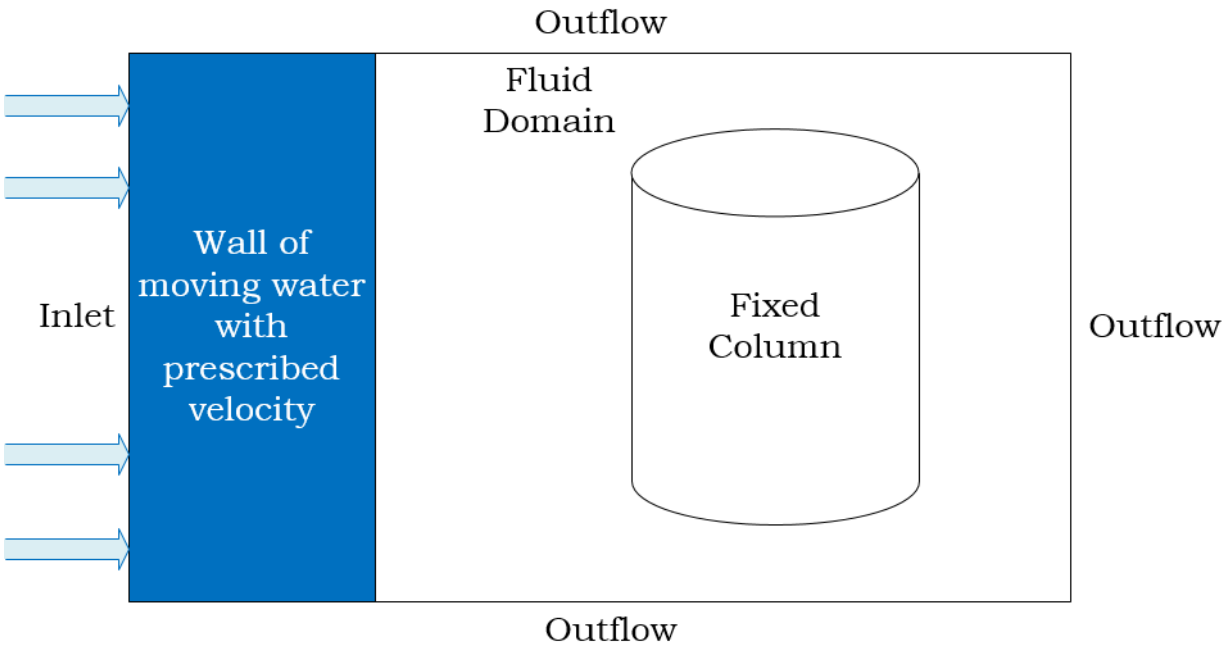

(a) First part of the simulation: water flowing through inlet

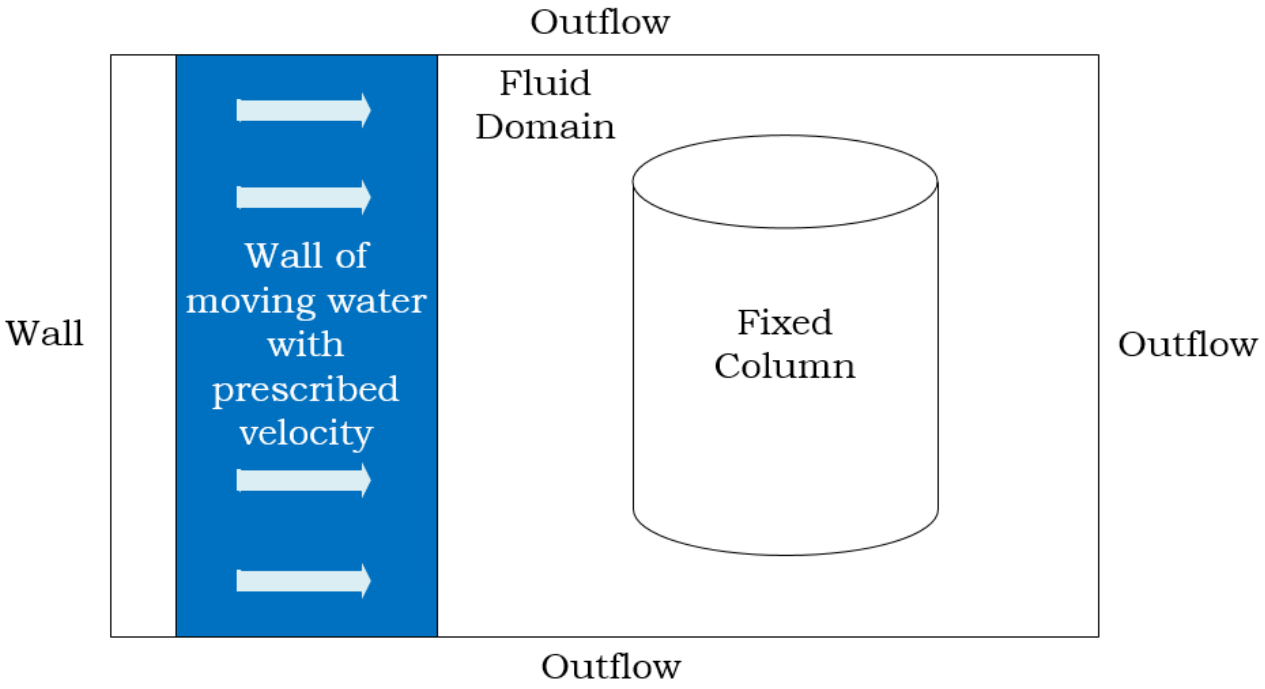

(b) Second part: inlet shut and replaced by a wall

Figure 3.1: Description of the simulation setup in the fluid solver

Chapter 4

Finite Element Modeling and Meshing

4.1 Geometric model of the column

The model of the column studied is based on an actual column of a semi-submersible platform. The column has a radius of 6m, and is composed of two concentric cylinders, with horizontal stringers and stiffened vertically. When it comes to the height of the column, the model is made to represent the zone where the slamming of the breaking wave actually occurs. DNV recommends to check for structural response on a zone representing a quarter of the wave height, over a section of 45°. Therefore, the model of the column has a height of 8m and the impact of the water occurs over a section of 7m centered on the model.

The column is made of two concentric shells stiffened horizontally by stringers and vertically by Holland-profile (HP) stiffeners in the inner sections and T-beams on the outer panel. The plan of the column stringers and the plan of the column between stringers can be seen on the Figure 4.1 and Figure 4.2. The stringers are evenly separated by 2m and divide the model in four sections.

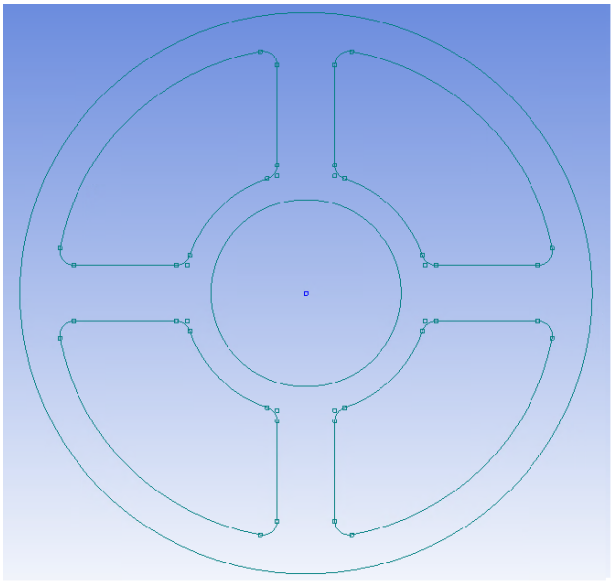

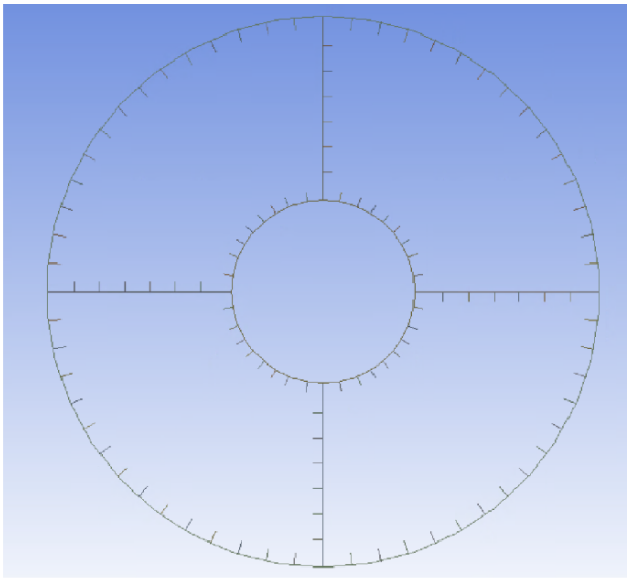

Figure 4.1: Plan of the column stringers (left) and of the column between the stringers (right)

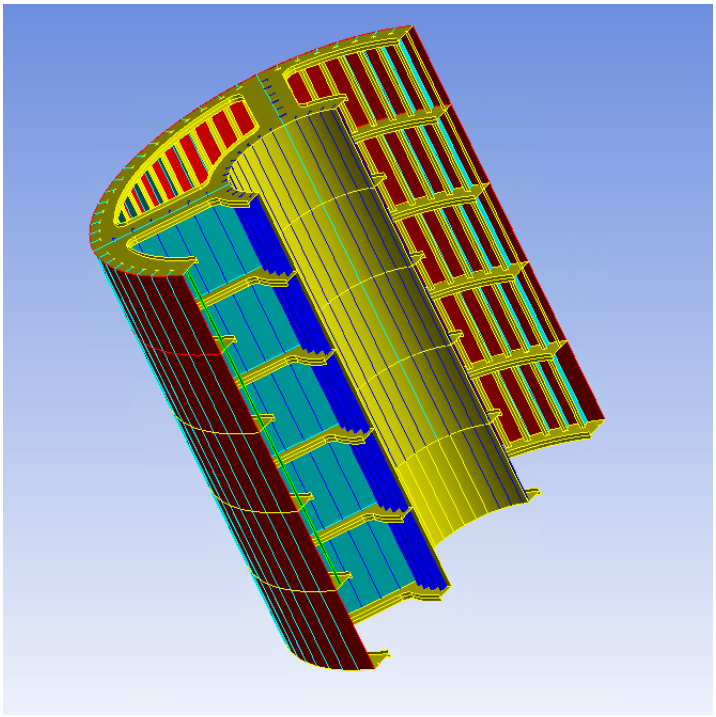

Figure 4.2: Cut view of the model of the column in ANSYS

4.1.1 Model members

Inner and outer shells

The main structural elements of the columns are the inner shell and the outer shell. They are concentric hollow cylinders of a diameter of 12m and 4m, respectively, connected by four 15mm-thick plates, see Figure 4.3. The outer panel, more subject to loadings is 30mm thick, the inner panel is 20mm thick.

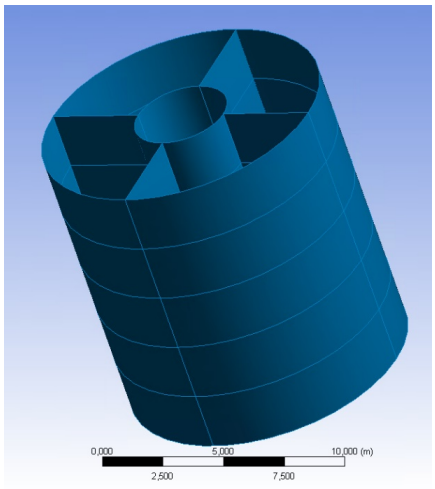

Figure 4.3: Geometry of the main shell elements

Stringers

The column is horizontally stiffened by girders with a thickness of 20mm and spaced by 2.5m. The free edges are stiffened with flat stiffeners of dimensions 200x20mm. The model is illustrated in Figure 4.4.

Stiffeners

Two types of stiffeners are used for the model. The outer column is stiffened vertically by 280x12mm T-shaped stiffeners. The dimension of the flange is 16x1.5mm. Each quarter of the shell is stiffened by fourteen evenly spaced members. The inner shell and the flate plates are using 200x10mm Holland-profile stiffeners. In order to model the bulb of the stiffeners, a simple shell offering approximately the same properties (moment of inertia, section of modulus) as the bulb is used.

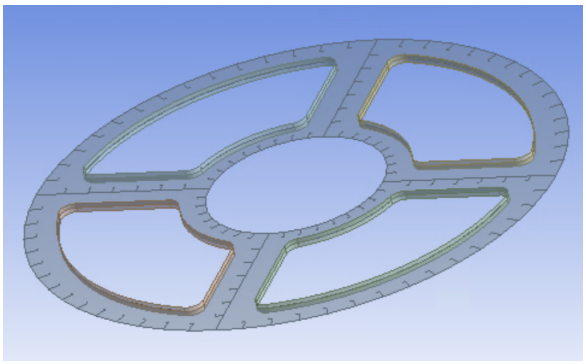

Figure 4.4: Geometry of a stringer

4.1.2 Material

The structure is using tructural steel grade S420 throughout all members. Structural steel S420 is often used for offshore structures for its high strength and good welding properties. The physical properties of the material are taken from NORSOK Standard CR-120 (NORSOK, 1994), see Table 4.1.

Table 4.1: Material properties

Properties	Steel grade S420
Yield stress [MPa]	420
Young's Modulus [MPa]	210 000
Poisson's ratio [-]	0.3
Density [kg.m-3]	7850
Ultimate Tensile Strength [MPa]	560

In order to simulate the elasto-platic behavior of the material, a multilinear isotropic hardening model is used with the values from (DNV, 2013) Recommended Practices C208. The stress-strain curve for structural steel grade follows a non-linear relationship illustrated in Figure 4.5. The structural steel used here has a clear yield plateau at σ = 560MPa.

The stress-strain curve illustrated here is obtained for a quasi-static loading. However, the loading during the slamming of breaking wave is characterized by a high pressure over time, making the quasi-static assumption obsolete. Haque and Hashmi (1984) showed that the strain rate has a great impact on the strain-stress relationship. Stress values obtained by dynamic tests are twice those for quasi-static strains of 0.1. Storheim and Amdahl (2015) also discussed the sen-

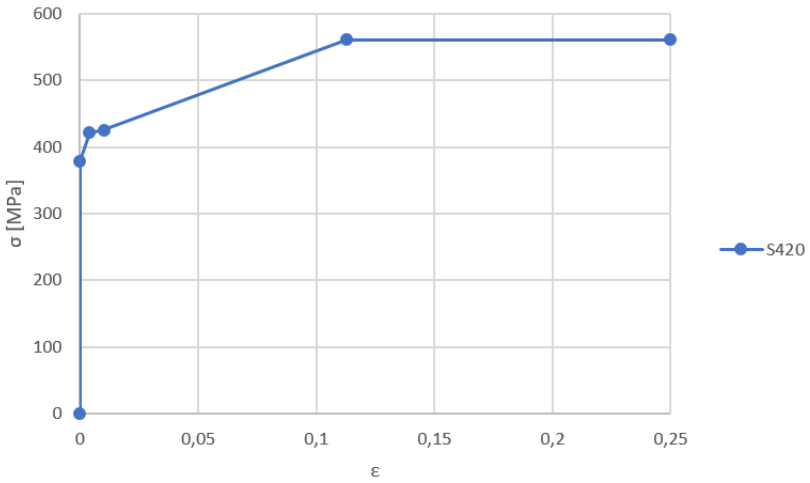

Figure 4.5: True stress-true strain curve for the steel used in the model

sitivity to work hardening and strain-rate effects in the analysis of ship collisions and show that the law used for both the work hardening and the strain-rate relations can have a very high influence on the energy dissipation and the residual plastic strain. These parameters are not studied in-depth in the current analysis, but as the phenomena mentioned above are strain-limiting effects, it only places the study on the conservative side.

4.2 Meshing configuration

Solid domain

An appropriate mesh sizes is fundamental in order to obtain good results. The stresses and strain concentrations can only be captured due to a fine mesh. The deformations can therefore be captured more accurately and the whole simulation benefits from it, as the deformation of the wall is transferred to the fluid solver in order to solve the fluid-structure interaction with a high precision. The mesh size is also linked with the computation time; a finer mesh leads to more elements and thus to a longer computation time. It is therefore necessary to simplify the mesh where high stresses and strain are not expected.

A way to speed up the computation time is to only use the relevant part of the structure. As much as the whole semisubmersible platform is not modeled for this structure because it is not

relevant, the three quarter of the column not exposed to slamming is not accounted for here. The boundary conditions are modified accordingly.

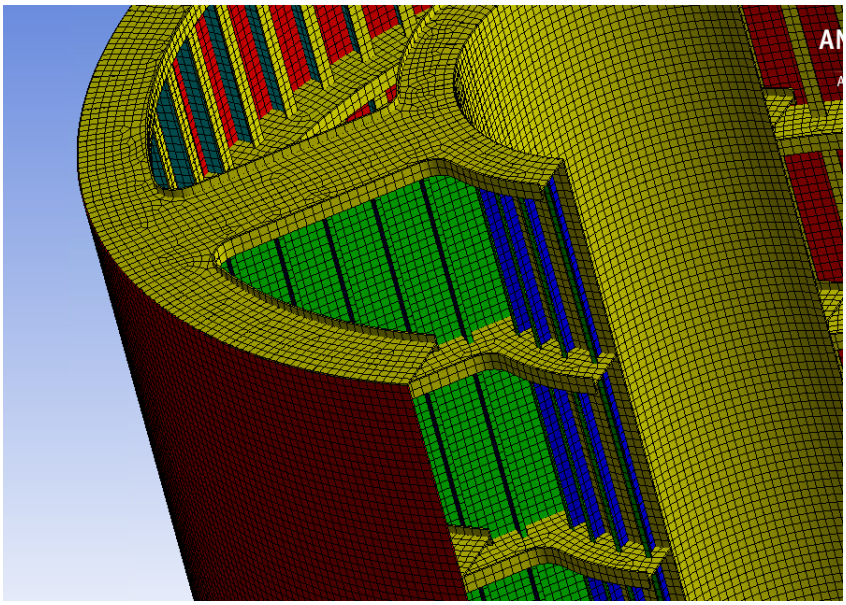

Figure 4.6: Mesh of the column model

The model is using shell elements for the whole structure. They are useful for thin-walled structures when one of the dimensions is very small compared to the two others. In the current case of stiffened panels, where stresses across the thickness of members is not of major importance, shell elements have several advantages. Good quality elements are easier to obtain with a shell mesh, leading to an overall higher stability and better convergence for nonlinear analysis. When it comes to computation time and disk space, using shell elements is very advantageous, especially for a coupled analysis generating a large amount of data.

The mesh uses quadrilateral elements with a low aspect ratio. The aspect ratio is defined by the ratio of the longest to the shortest side of an element. Ideally, a mesh should be composed only of elements with an aspect ratio of 1, defining only squared elements. This low ratio is obtained for regular surfaces, such as the stiffeners, the inner and outer shells. However, for more complex geometry, for example the girders, squared elements cannot be created, but the aspect ratio should stay low. Some triangular elements have to be used when quadrilaterals are not applicable. The structural domain uses quadrilateral shell elements over the domain. A uniform sizing

is used all over the body, with the ideal element being a square with sides of 0.1m, see Figure 4.6. Different properties attesting of the quality of the mesh can be seen in Table 4.2. The element type used in ANSYS Mechanical is SHELL181, which can be used for both thin to moderately-thick shell structures. Elements are four-noded and account for shell thickness changes during non-linear analyses.

Table 4.2: Element properties of the model

Number of elements	Total	92871
	Quad	92681
	Tri	190
Element Quality	Average	0.97
	Std Deviation	0.05
Aspect Ratio	Average	1.1
	Std Deviation	0.14
Skewness	Average	0.02
	Std Deviation	0.06

Fluid domain

The fluid fluid domain surrounding the structure is rectangular cuboid of dimensions 7.2×14.6×14m. The faces of the domain are meshed with triangular elements of size 0.2m. The general fluid domain mesh is set to 0.3m tetrahedrons. However, the face corresponding to the fluid-solid interface is refined to 0.1m triangles. An inflation algorithm is employed around the inside walls corresponding to the structure. 7 layers of hexahedrons with a growing factor of 1.2 are used at the interface of fluid and solid domains in order to achieve a higher accuracy of the fluid action on the body, for a total thickness of 0.2m, see Figure 4.7. The inflation layer is set to deform accordingly with the fluid-solid interface. 610,504 elements with an average skewness of 0.23 compose the fluid domain.

As the simulation uses a two-way coupled system, the boundaries of the fluid mesh are deformed according to the structural deformations. Therefore, the mesh needs to be remeshed at

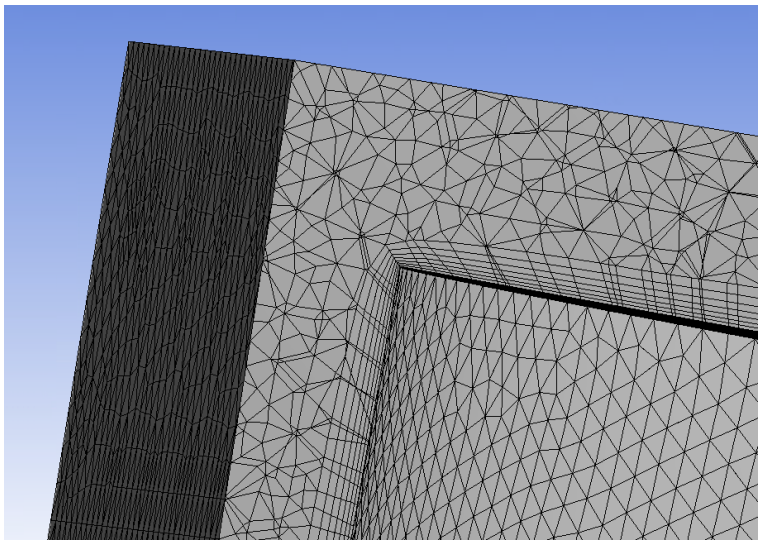

Figure 4.7: Close-up view of the inflation boundary layers around the body

regular time intervals in order to avoid having highly skewed elements around the solid domain boundaries.

4.3 Boundary Conditions

Selecting the appropriate boundary conditions is a challenge in order to get results that correspond to the real situation. The conservative solution is to use fixed boundaries at every node. As Figure 4.8 shows, the sections B represent the nodes where the circular sections are cut. The edges located in this plane are simply supported:

- $U_x = 0, U_y = 0, U_z = 0$
- The moment at the nodes of those edges are null

Where U represents the translations along the axes.

The nodes along the top (see section A) and bottom sections of the column are also simply supported. The boundaries are located 0.5m away from the zone of impact with the fluid. When considering the whole column, the nodes at the extremities of the model would be located on stringers. Using fixed boundaries could be non-conservative as it would not account for potential deformations of the girders. Moreover, fixed boundaries can over-constrain the model

and the large loading from the slamming event can make the simulation fail due to convergence difficulties.

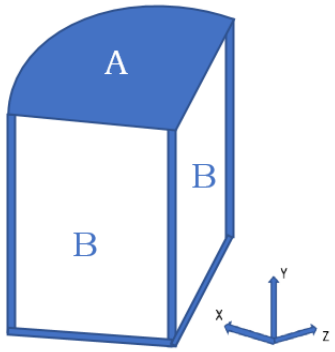

Figure 4.8: Drawing of the boundary conditions

These boundary conditions restrain the body from any rigid body motion. In the real configuration, the platform is not exactly fixed but is it assumed that the impact of the global movement of the structure is low, especially during a very short time duration.

4.4 Loading

The model does not account for any pretension or axial loading, as it would be in a real life configuration. The only load applied on the structure is the fluid force acting on the outer panel.

Chapter 5

Analysis of stiffened panels

In a first approach, a simple model of a stiffened plate will be used. In order to assess the impact of hydroelasticity on the slamming phenomenon, both a one-way and a two-way fluid-structure interaction coupling are used. The difference in pressure history, stress and strain will be discussed. All parameters besides the geometry and the mode of coupling remain the same in all the experiments.

5.1 Geometry and meshing of the model

The stiffened panel used for the simulation corresponds to a section of 90° of the outer column of the column between two stringers, see Figure 5.1. The dimensions of the different members are the same as those presented in Section 4.1. The analysis is carried out with a time step size of 0.1ms, which is a small enough time step to catch rapid variations in hydrodynamic forces. The meshing uses the same mesh size as the full model, with quadrilaterals of dimensions 0.1m x 0.1m. When it comes to the fluid domain, the same parameters as the full simulation are also used.

The panel is simply supported along every edge. As this does not reflect the actual boundary conditions of the panel in the full column configuration, the results cannot be extrapolated to the behavior of the panel as a member of the column.

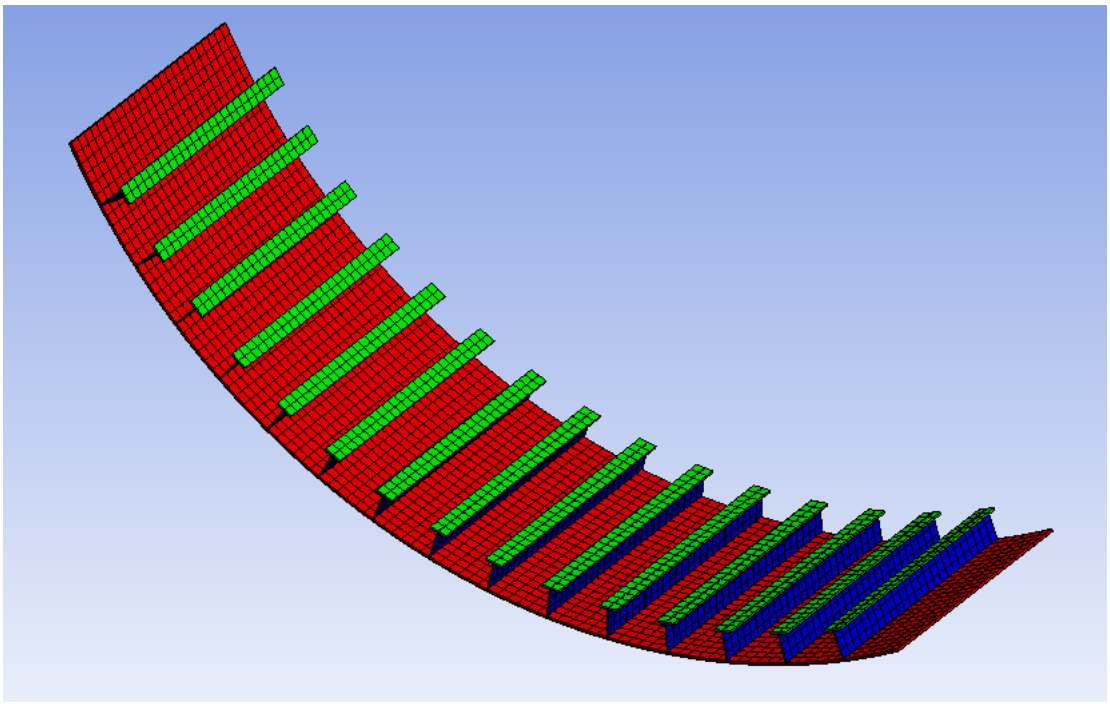

Figure 5.1: Model of the curved stiffened panel

5.1.1 Results of the one way coupling

Hydrodynamic loading

As expected by the setup of the analysis, the peak pressure rises and peaks around 0.045s, see Figure 5.4. The structure is located at 1m from the inlet, so the theoretical moment of impact is 0.0454s. The peak pressure is therefore obtained precisely at the moment of impact. The peak is sudden and local high pressures can go as high as 22MPa. But as seen in Section 2.5, local peaks of pressure are not a sufficient value in order to determine the response. The high pressure values are found on a very short time period and travel quickly along the body, the highest pressures are found within 15ms after the impact. The maximum pressure then drops rapidly and then stabilize at a roughly constant value of 2.5MPa. This plateau corresponds to the hydrostatic pressure of the flow acting on the panel. The graph represent the absolute maximum pressure on the panel at any time, however, the maximum pressure stabilizes 60ms after water entry which is before the whole panel has been hit by water. 60ms after impact, the water has traveled $d = 22 \times 0.045 = 1m$. At that level, the deadrise angle α (see Figure 5.2) is found by:

$$\alpha = cos^{-1}\frac{R-d}{R} \tag{5.1}$$

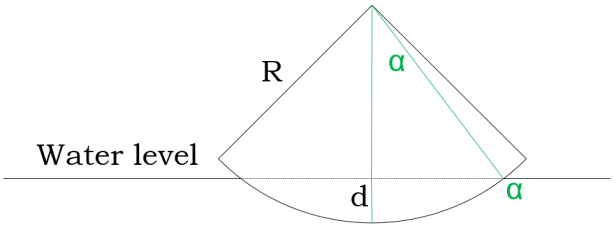

Figure 5.2: Drawing of the geometry to find the deadrise angle

We find $\alpha = 34°$, which means that over this value of deadrise angle, the shock pressure is not significant compared to lower deadrise angles.

The velocity profile during the slamming phenomenon shows that the fluid velocity in the jets in extremely high. The highest value is obtained less than 2ms after impact, with local velocities reaching 490m.s^{-1} close to the center of the panel. Figure 5.3 shows the velocity profile in cut view along the middle of the plate. In the later stages of the impact, 100ms after water entry, the velocity profile is closer to a typical fluid flow around a body, with a local velocity null in the center of the plate.

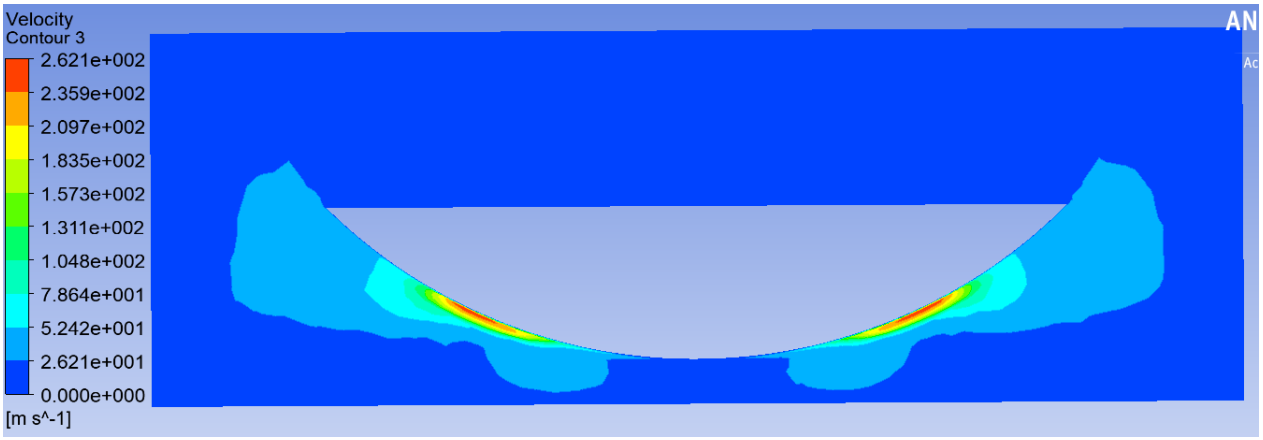

Figure 5.3: Velocity contour around the panel 15ms after impact

The extremely high velocity along the body is a result of the characteristic shape of the flow during slamming with run-ups and jets along the body, a snapshot of the early entry stage can

be seen in Figure 5.5. When plotting the contour of the pressure on the panel after impact, the highest pressures are found in the roots of the sprays. However, the total pressure on the areas that were impacted shortly before falls quickly close to the static pressure. It shows that the hydrodynamic slamming pressure decreases rapidly with time, see Figure 5.6. The panel is completely submerged by the panel 0.176s after the moment of impact. However, due to the run-ups and the jets, high pressures occur on the panel extremities only 25ms after water entry. The maximum value of pressure is 22MPa, reached only 1ms after the impact, which is in accordance with Figure 5.4.

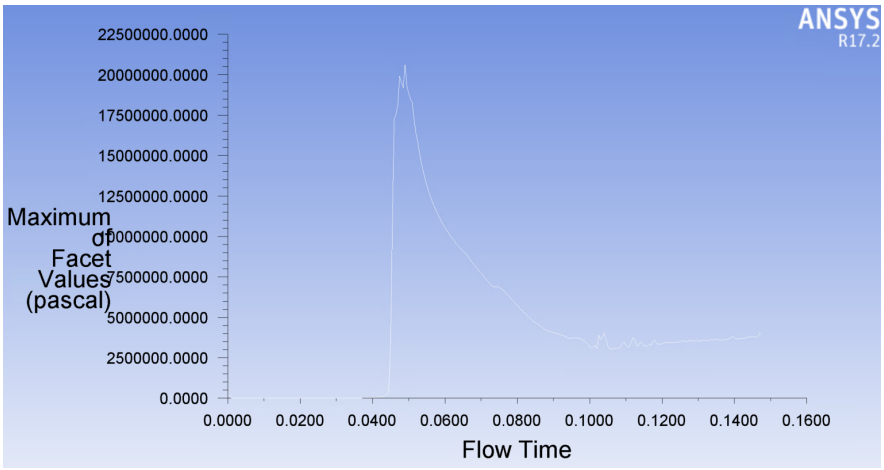

Figure 5.4: Plot of the maximum pressure on the panel over time

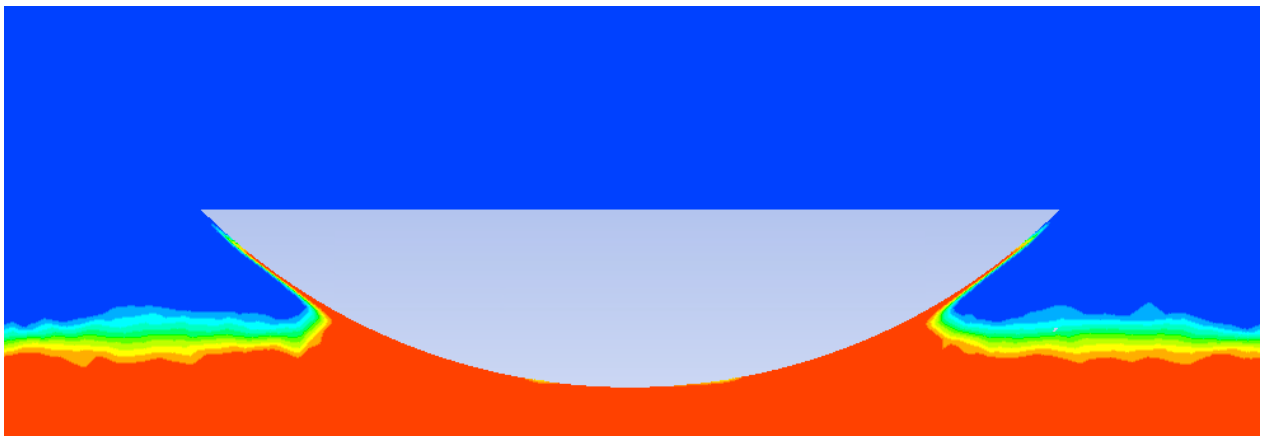

Figure 5.5: Snapshot of the flow 20ms after impact

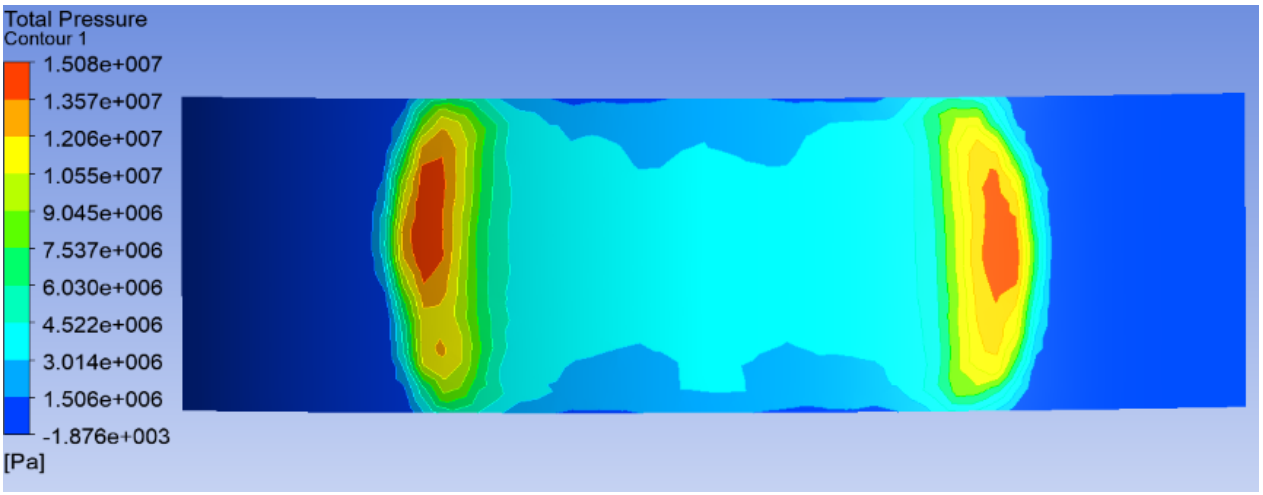

Figure 5.6: Pressure contour on the panel 20ms after impact

Structural response

The first important result to notice is that the deformation of the panel is high, with a maximum lateral deflection of the panel of more than $400mm$. This is the results of the extremely high forces acting on the panel, specifically during and shortly after the impact moment.

In Figure 5.7, we can see the stress distribution on the panel on four time steps within 0.03s after the impact. The stress concentration is especially high around the center of the plate, where the deadrise angle is close to 0°. The stress reaches a peak of 560MPa immediately after the the entry in the water. This value of stress is higher than the yield stress and thus leads to plastic straining. We can see a stress front propagating along the panel, which coincide with the water run-ups on the plate. The stress stays high on the panel in the center even after the actual impact due to the high velocity of the fluid, around ultimate strength level even 60ms after impact (Figure 5.11a). The 3 central stiffeners are the ones particularly affected by high stresses, with ultimate strength magnitude in their middle.

The very high lateral loading and thus stresses lead to a large strain. Two types of strains can be described, elastic and plastic strain. Elastic strain is the strain caused by stress which are below yield stress, while plastic strain is caused by higher stresses. The maximum total strain is located at the stiffeners boundaries and reaches a maximum value of 0.45 only 60ms after water entry.

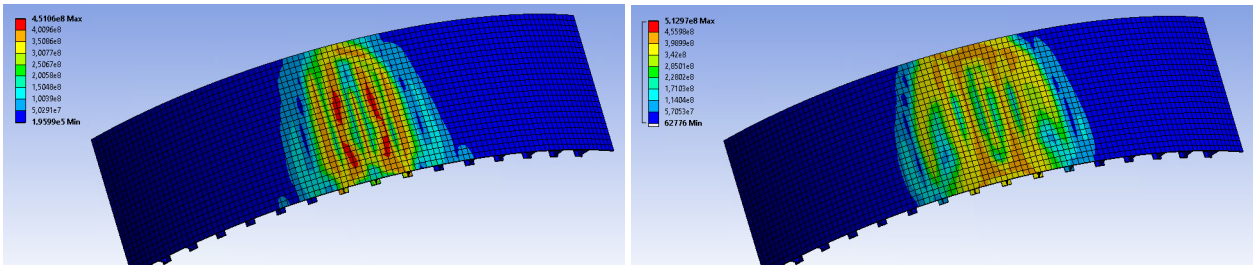

(a) $t = 0.001s$ (b) $t = 0.002s$

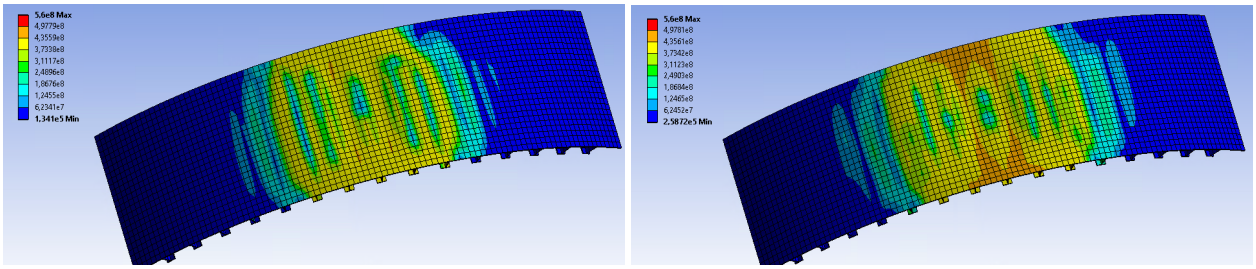

(c) $t = 0.003s$ (d) $t = 0.004s$

Figure 5.7: Plot of the Von Mises Equivalent Stress over the surface of the panel at different times after impact [Pa]

NORSOK gives a value of critical strain for steel grade S355 $\epsilon = 15\%$, however it is a design value and the actual material's rupture strain is usually above 20% (Wang et al., 2005). A high value of strain such as the peak found in the results can lead to failure, but it is very located in space as illustrated in Figure 5.8 indicating that the damage from this is not a major concern. The residual strain on the panel never exceed 20%, and is almost everywhere lower than the 10%, see Figure 5.9, the same goes for stiffeners, where the residual plastic strain is below 15% except for the localized high strains close to the boundaries.

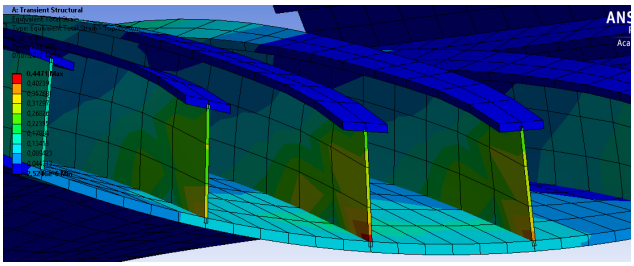

Figure 5.8: Strain concentration at the base of the stiffeners

The elastic strain goes to 0 after the impact, which means that the drag force is not sufficient to

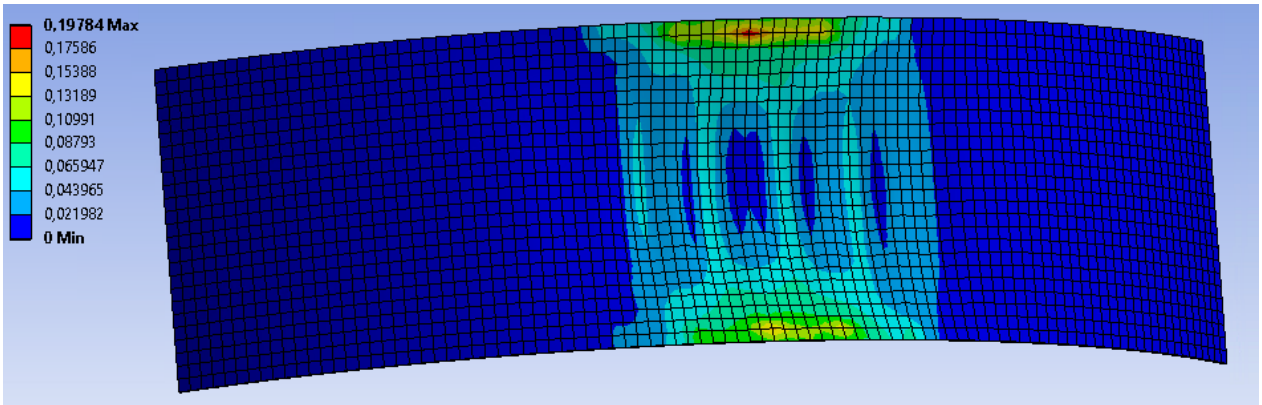

Figure 5.9: Residual strain contour on the panel

deform the impact and proves that the damages on the structure are solely caused by the slamming impact. However, high elastic strains can be dangerous for the structural integrity during water entry, as it can lead to tensile failure of an element. The plastic strain is residual, which means that it is the permanent deformation that will remain in time.

When it comes to deformation, a side shell deformation of 50-75mm is considered as structural damages that need to be repaired immediately (Hong et al., 2009). The values obtained here are largely above these values, as the maximum lateral deformation of the panel is of 424mm. The value is dangerously high and even though tensile failure is not of major concern due to the strain, the load bearing capacity of the column could be at stake with such a large deformation. However, the deformation is localized in space, with a sector of less than 30° being subjected to more than 50mm of lateral deformation. This supports the assumption made based on the interpretation of the plot showing the maximum pressure that higher deadrise angle are subject to lower peak pressures, that are not sufficient to create plastic strain on the panel.
In the later stage of the slamming event, the plate displays vibrations in the impacted area. Figure 5.12 shows that the maximum lateral displacement on the panel is varying in time after reaching its peak. The plate is therefore vibrating in its middle where plastic deformation have occurred. These vibrations are of low amplitude and a period of 3ms (~ 333Hz), a few millimeters, and dampen quickly.

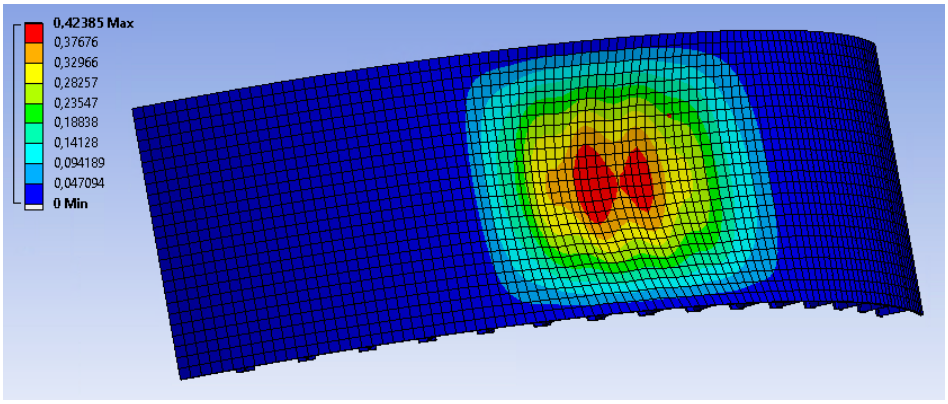

(a)

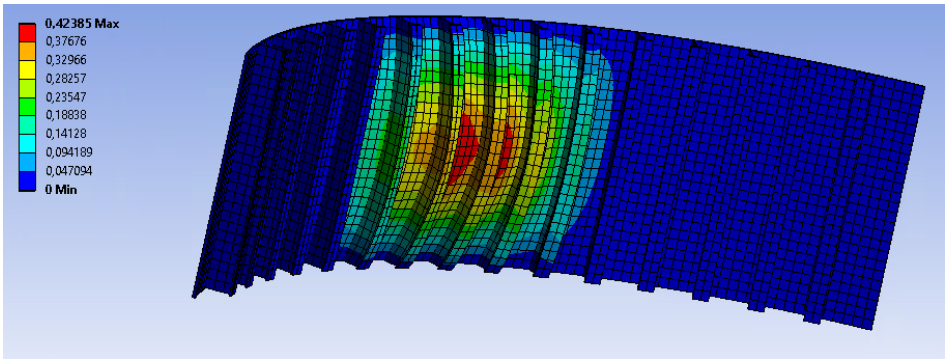

(b)

Figure 5.10: Contours of the residual lateral deformation on the panel due to slamming [m]

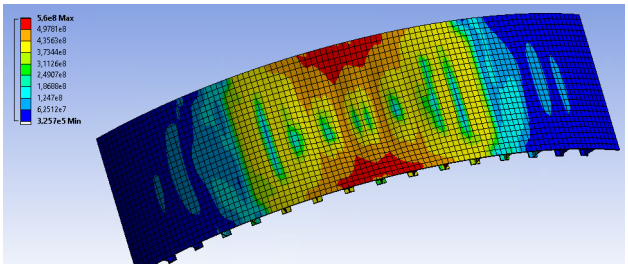

(a) Contour of the stress on the panel

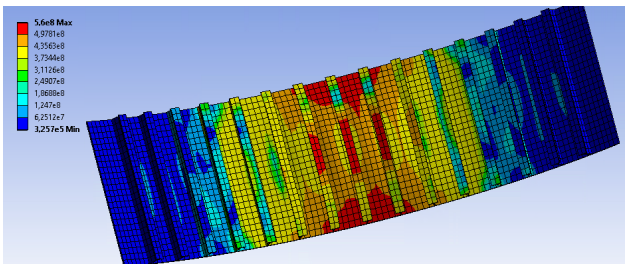

(b) Contour of the stress on the panel and stiffeners

Figure 5.11: Stress contours on the model 60ms after impact [Pa]

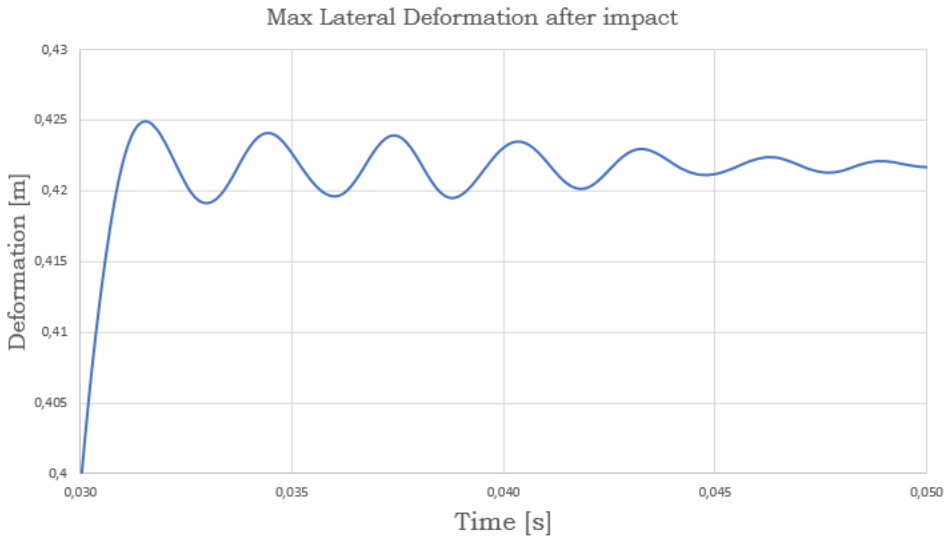

Figure 5.12: Plot of the maximum lateral deformation on the panel after impact showing the vibrating pattern of the structure

5.1.2 Results of the two way coupling

Hydrodynamic loading

In terms of loading, the two way coupling offers values significantly lower than the one way coupling. The use of a deformable panel reduces greatly the peak pressures reached with a rigid body. The deformable panel only reaches a maximum of 10MPa. The slamming impact in itself is therefore less violent for a deformable panel all along the body than it could be expected. However, the magnitude of pressure 15ms after the impact is almost the same as previously, but the panel deformation during the simulation offers a particular asymmetry to the pressure contours, as illustrated in Figure 5.13. The high dynamic pressures caused by the sprays are also found.

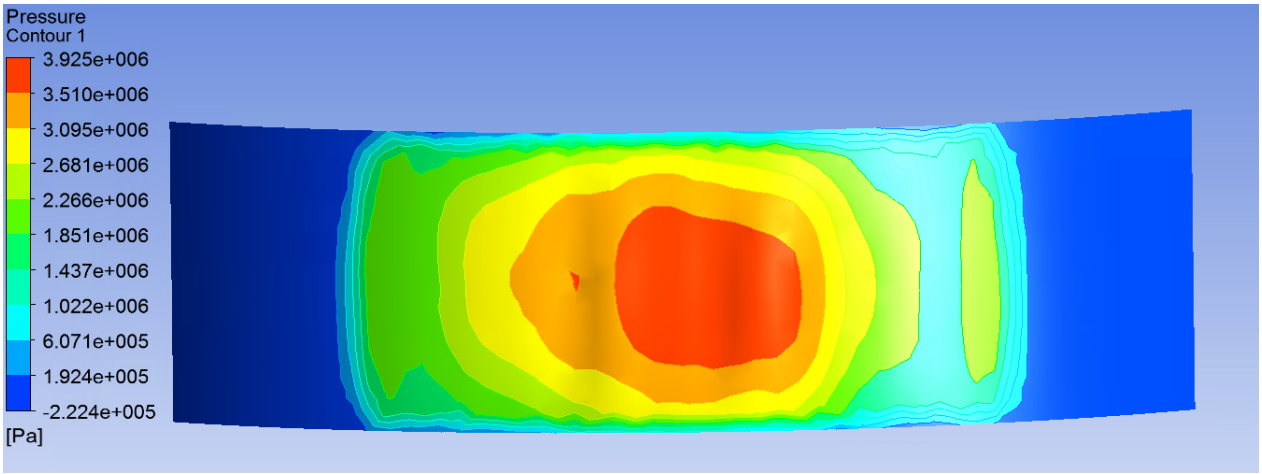

Figure 5.13: Hydrostatic pressure contour on the panel 20ms after impact. The deformation of the panel makes the flow and the pressure asymmetric.

Structural response

The first simulation suggests that the very moment of impact and a short while after is the significant time period for the deformation to occur on the structure. The relatively lower impact pressure leads to significantly less stress concentrations and peaks in the structure. As a result, the Von-Mises stress in the panel never goes above 462MPa, which is less than 10% above the yield stress of the material. It however remains above the yield stress during the whole impact, which leads to residual straining. Only 15ms after the impact, the deformation of the panel is

already large and one can see the large stress concentration in the area where the lateral deformation is important, see Figure 5.14.

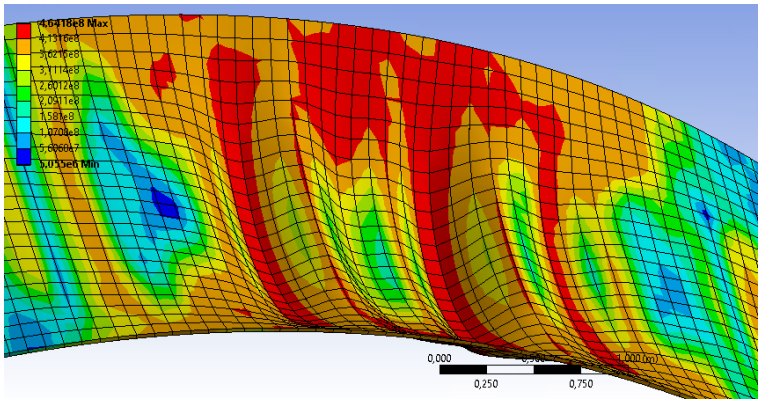

Figure 5.14: Stress concentrations in the zones of large deformation (deformation is scaled 3.3 times) [Pa]

The relatively low stress on the panel is directly linked to the relatively low strain. The maximum plastic strain in the structure is located at the bases of the central stiffener, but the maximum value is 17%. When it comes to the rest of the model, the panel gives a maximum residual strain of 5.5% as seen in Figure 5.15, reached less than 20ms after water entry. The overall strain in the structure during the slamming is not of major concern for failure.

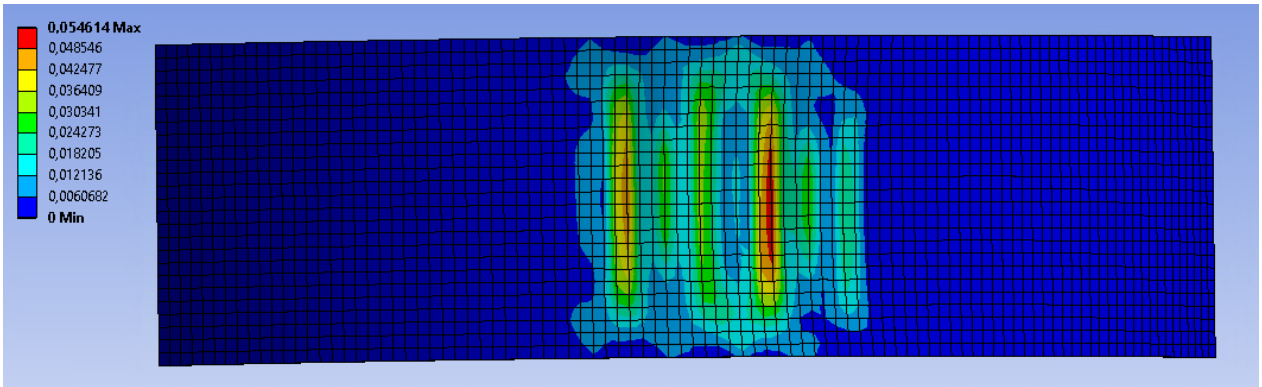

Figure 5.15: Residual strain contour on the panel

The lateral deformation of the structure after the slamming impact is large. It reaches a maximum of 193mm close to the center of the panel, with values above 50mm over a section of 30°

centered in the middle of the plate. The stiffeners tend to minimize the deformation, as the maxima are reached in the area between two stiffeners. The plot of the maximum deformation over time is illustrated in Figure 5.16b.

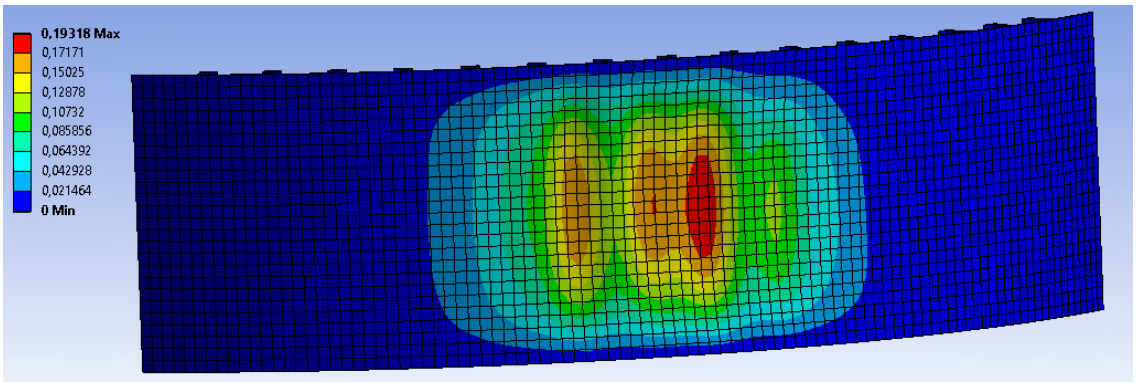

(a) Contour of the residual deformation on the panel [m]

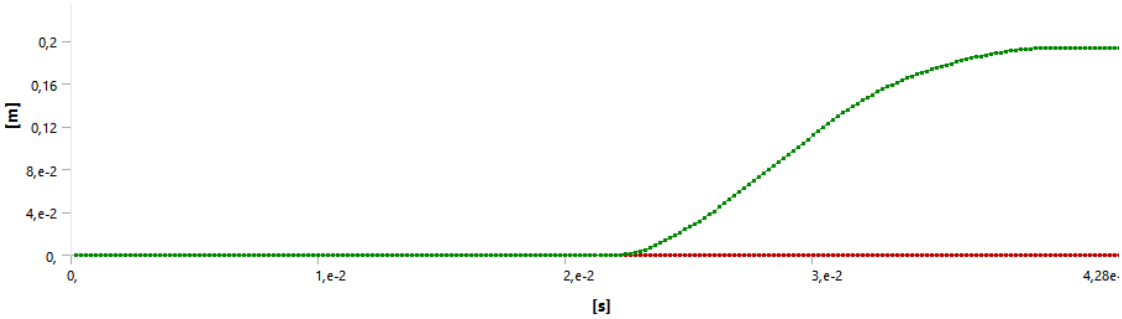

(b) Graph of the maximum deformation on the panel over time

Figure 5.16: Characteristics of the deformation on the panel during the slamming impact

5.2 Comparison of the two different methods and discussion of the results

The main difference between both methods is essentially the uses of different stiffness for the fluid solver. The first simulation use a rigid body and thus does not account for hydroelasticity in the experiment. The second uses a panel that deforms over time and the fluid's boundaries are modified at the same time as the structure deforms. This leads to the inclusion of hydroelastic effects, which, as Bereznitski (2001) showed, can reduce the deformation of the structure during slamming up to 75%. At the moment of impact, a part of the energy is dissipated by the straining of the structure, which leads to a reduced pressure. An extended study of the deformation and

maximum strain over time for both simulation shows that the damages on the structure occur significantly quicker for the one-way coupling than the two-way coupling, see Figure 5.17. The maximum is reached less than 10ms after impact for the one-way and more than 15ms after water entry for the two-way coupling. These values and the pressure history from Figure 5.4 are of the same order of magnitude as the value given in Eq. 2.18, although slightly higher. Both major effects of hydroelasticity are therefore illustrated with those simulations:

- *Reduction* of water pressure and more moderate structural response
- Distribution of the load over a *longer* time period

Moreover, the one-way coupled plate displays small oscillations in its center. Vibrations of comparable amplitude are not found for the simulation including the hydroelastic response of the plate. The effect of added mass can explain the absence of significant vibration in the second simulation. As the structure is deforming and oscillating in the fluid, it needs to accelerate the surrounding water, meaning that the structure applies a force to the fluid. From Newton's third law, the fluid in return applies a force of equal magnitude on the structure. Added mass can reduce the amplitude of oscillation by *virtually adding* mass to the structure and modifying the natural frequency of the structure (Muren, 2016). Another value which is interesting to compare

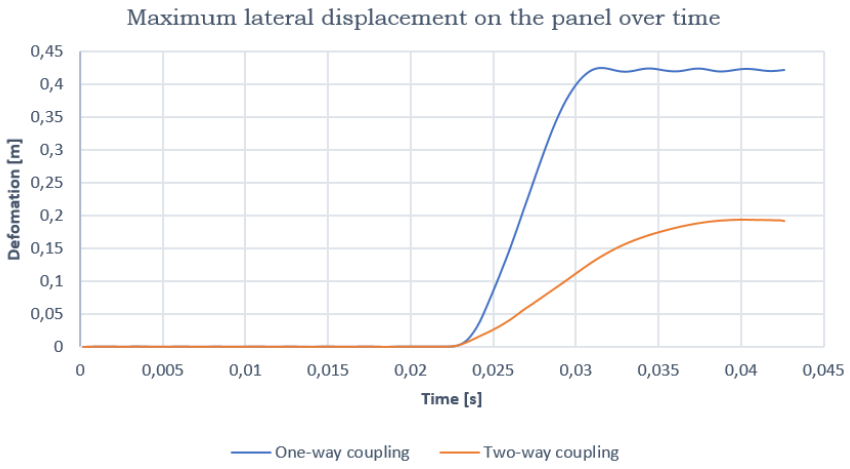

Figure 5.17: Graph comparing the maximum deformation over time for both simulations

is the deformation speed of the structure. Figure 5.18 shows the comparison of maximum lateral speed of the structure for both simulations. We can see that both structures are subjected to a

high acceleration at the moment of impact, but the curve flattens quickly for the two-way coupled simulation, reaching a maximum of 20m.s^{-1}, while the one-way coupled panel has an area with a lateral speed peaking at 70m.s^{-1}. This can be explained by the reduced pressure for the second simulation, as the plate boundaries are updated in real time, leading to a lower velocity differential between the panel and the fluid.

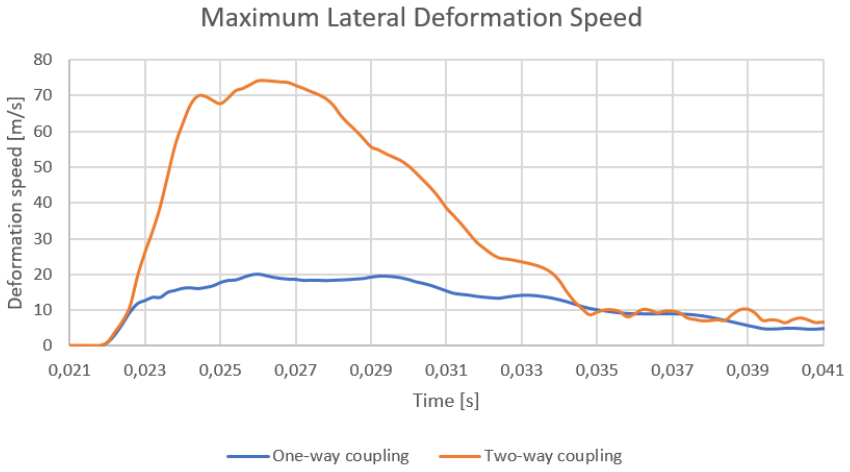

Figure 5.18: Graph comparing the maximum deformation speed over time for both simulations

The results of both simulations are summarized in Table 5.1.

Table 5.1: Summary of responses

		Max Residual Strain [%]	Max Deformation [mm]
One-way coupling	Panel	20	193
	Stiffeners	45	165
Two-way coupling	Panel	5.5	422
	Stiffeners	17	376

The results show that model tests in basin may lead to over-conservative results with higher than actual water pressures. While the residual deformations from the first simulation are non-acceptable and can be very dangerous for the structure, the two-way coupling shows a more moderate and acceptable response of the structure to extreme slamming loads. The two-way coupling is therefore required for accuracy, and hydroelasticity is the main reason for this. However, these simulations represent only a small section of the platform's column and a more complete simulation has to be carried out in order to assess the structural integrity of the platform

in case of an impact with a wave corresponding to the ALS conditions. The boundary conditions used for the simulations are certainly too restrictive when it comes to lateral deflections, because they are acting as if the stringers were rigid body. This is also the cause of the high strain concentrations close to the edges of the stiffeners.

Chapter 6

Coupled simulation of the slamming impact on an offshore platform column

This chapter describes and analyzes the results of the slamming event on the column platform.

6.1 Modification of the simulation

Unfortunately, it was not possible to carry out the simulation with the full model and a perpendicular impact. The limitation in the calculation capacity and time limit made it a challenging task to fulfill. Only partial results are available for the simulation on the column. Simulation slamming on a cylinder, as it has been seen in 2.5, is computationally challenging due to the numerical singularity at the point with a null deadrise angle. The first problem arising when analyzing the slamming problem with a system coupling is the structural domain. The complex structure comprises many contacts between parts and the force convergence is hard to obtain in the mesh elements that are directly exposed to the slamming loads. A recurring problem obtained is the non-convergence in the structural solver due to a load ramping too quickly and a time stepping too high. While the parameters described in Chapter 4 are used and give relevant results for the simple analyses, the computations could not be achieved the same way for the whole column. Nonlinear problems have residual force imbalances that are harder to reduce the more complex the geometry is. With a time step as low as $\Delta t = 2 \times 10^{-5} s$, the solution was still unable to converge. Moreover, the fluid solver is also causing diverging patterns. The defor-

mations to the panel caused by the fluid flattens the cylinder and makes it similar to a flat wall, which causes a large area to have a deadrise angle close to 0. The pressure rose to values which are too high and not physically acceptable. Tests carried out showed that the solver was diverging within reasonable range of mesh sizing and time stepping in the case of slamming when the fluid is perfectly perpendicular to a flat plat.

A solution is therefore to have extremely fine time steps and mesh size. However, the computation of a single time step for the model described in Chapter 4 was close to 600 seconds. When reducing the time frame to 30ms to capture only the most important part of slamming, it can still lead to weeks of computation, which is not a possibility in the period allowed for this work. Moreover, Larsen (2013) showed that reducing the time step size during the water entry tends to increase the peaks of pressure acting on the body, thus making the structural domain even harder to converge.

Due to the reasons mentioned above, the simulation could not be carried for the configuration of a horizontal impact. The cylindrical column is inclined with an angle of 7.5°, which certainly reduces the slamming load but is a configuration that can be found in a real event of a wave breaking. As previously described, the overturning moment of the breaking wave is particularly difficult to predict, when also taking into account the heeling angle of the platform, which can be up to 6° (Voogt and Soles, 2007). All other parameters are conserved. The simulation layout can be viewed on Figure 6.1 prior to the impact.

6.2 Water entry of the column

Due to the inclined configuration, the water front does not hit the whole length of the column at once. On the contrary, a progressing pressure front can be seen at the location of impact, as illustrated in Figure 6.2. The maximum pressure is gradually increasing with the surface in contact with water, reaching a maximum of 26MPa, but as seen in Figure 6.2b and 6.2b, the duration of the high pressure peak is less than 12ms. The high pressures caused by the sprays

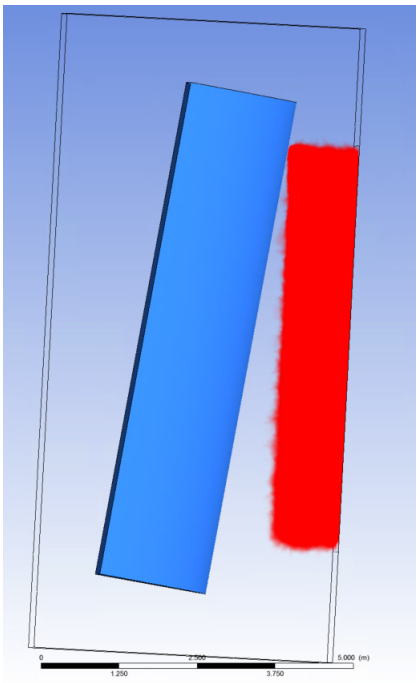

Figure 6.1: Representation of the simulation 2ms before water entry. The water is represented by the red domain.

are clearly visible in the pressure contours.

6.3 Structural response

As the pressure contours highlighted, the pressure at the location where the column first touches the water sees a quick rise and decay, and extreme values lower than those found in the middle of the column. No residual deformation can be found close to the top of the water domain. On the other hand, some significant deformations are found closer to the middle of the column. The deformed shape of the panel shows the influence of supporting members, in fact, the deflection is larger between two consecutive stiffeners, see Figure 6.3. This gives the panel a particular shape with a succession of troughs between stiffeners. Regarding the stringers, their curved beam shape confer them a large bending moment, which leads to a high resistance to the loading applied. Effectively, the maximum deflection of the middle stringer is 20mm, which is less than half of the maximum deflection of the panel (45mm). The study of the evolution of maximum velocity and deflection of a part of the panel between stiffeners shows that the maximum deformation is reached 20ms after this part of panel is first hit by the water, and no more

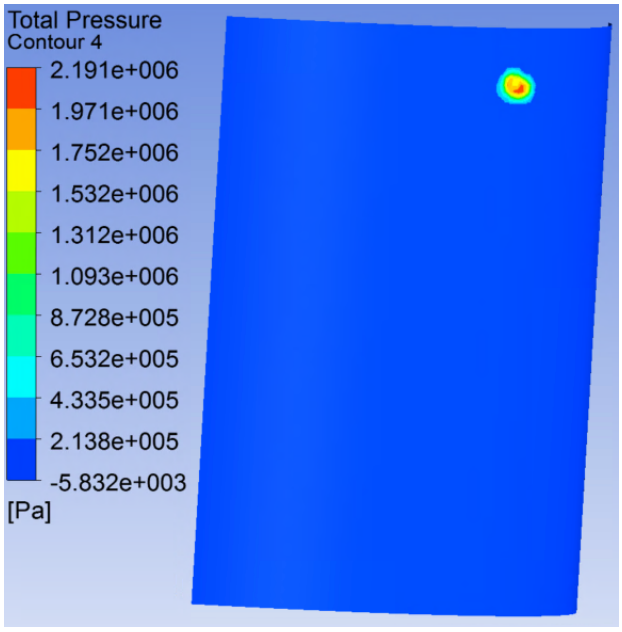

(a) Moment of impact with the water, $t = 0s$

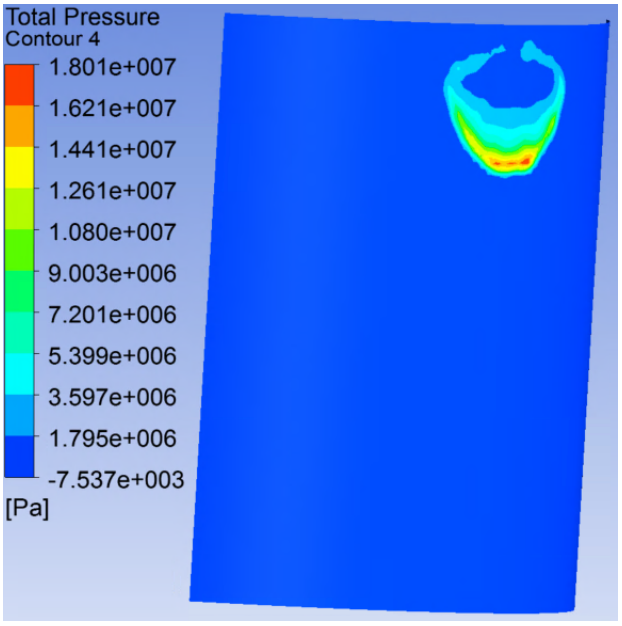

(b) $t = 6ms$

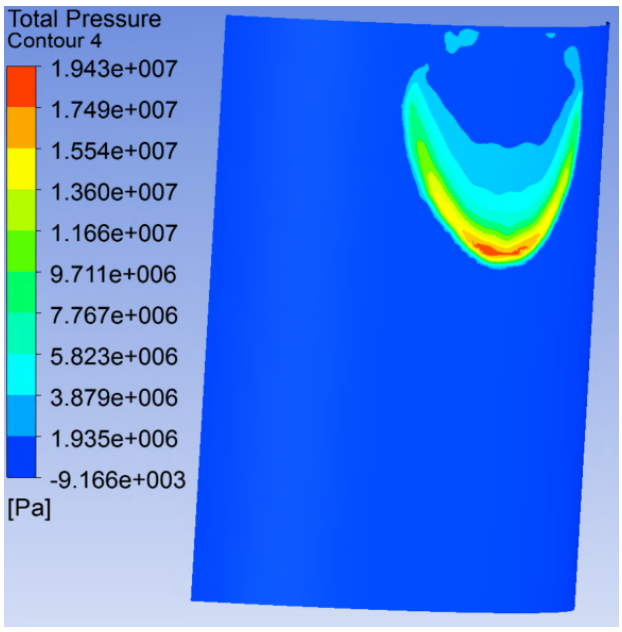

(c) $t = 12ms$

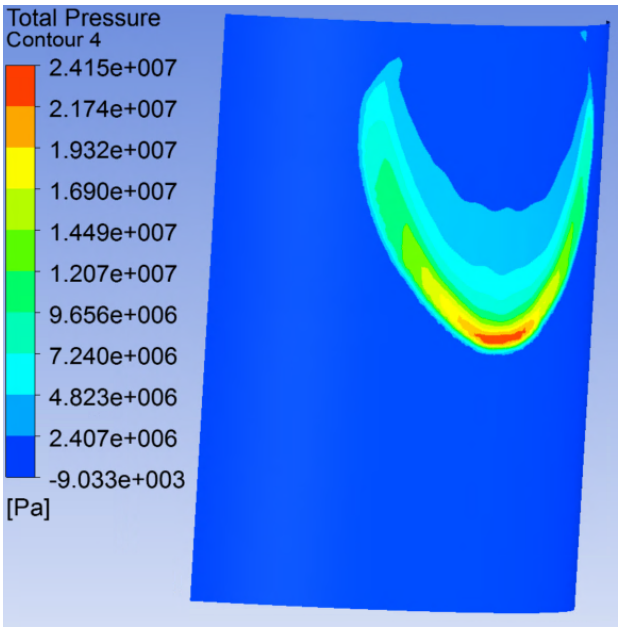

(d) $t = 18ms$

Figure 6.2: Pressure contour on the body showing the progressive water entry of the column

significant deformation is found later in the water entry stage.

The analysis of the stress in the structure reveal streams of high pressures corresponding to the sprays along the body. The stress values are equal to or beyond the yielding threshold on several areas of the panel and on the central stiffeners, reaching up to 460MPa. Figure 6.4 shows the equivalent stress in the central stringer and the stiffeners. The central part of the stringer is not affected by high stresses, however, stress concentrations occur close to the corners. Large bending stress is found in the flange of stiffeners. The area that is most exposed to high stress is the along the median line. As a result, residual strains are present on the structure. Plastic straining happens 4ms after the moment of impact and gradually increases as the water front progresses along the column. Residual straining on the panel are of 2% on the most impacted areas, while it is below 1% for internal members. The plot of the evolution of the maximum plastic straining over time on one section of the panel is displayed in Figure 6.5; the value reaches a maximum 14ms after the first straining occurs.

6.4 Analysis of the results

In this chapter, the slamming of a wall of water on an inclined column was assessed. Unfortunately, only partial results were obtained but they give an interesting insight on the behaviour of a platform column subjected to such an event. That the impact can cause residual deformations, which are potentially weakening it for future events. Moreover, high stress and strain concentrations are found on stiffeners and close to contact points with other members, which in real structures are welds. Welds are prone to stress concentration and crack initiation (Gurney, 1979) and a violent impact is likely to initiate cracks. Repeated impact of this magnitude, but also slamming impact of lower magnitude, lower the fatigue life of the structure significantly(Thomas et al., 2006). With residual straining up to 2% on the panel, denting occurs between supporting members, but it is not a direct threat to the integrity of the structure as the rupture limit is generally one order of magnitude higher (Wang et al., 2005). Considering the rarity of events of this magnitude, it is not unreasonable to allow side deformations to a certain degree, although structures should be checked for potential more serious damages. A criterion

of allowing one time the plate thickness as permanent deformation was suggested by Wang et al. (2002); in the current study, a maximum of 1.5 times the shell thickness was found. However, this criterion refers to bows of FPSOs under recurring slamming forces, but the slamming simulated in this work is due to a wave with a height recurring once every 10,000 years, so the area of impact is high above the mean water line and is unlikely to suffer many impacts during the operating life of the platform.

The low to null stress on members not close to the impact shows that the reponse of the column in purely local, and no global deformation has to be accounted for, but primary structural members are also subjected to important loads, including stringers and stiffeners of the outer shell. The internal stiffeners however are not subjected to any significant stress. The impact being very localized and transient does not allow the structure to have a global answer to the shock. This validates the choice of reducing the geometric model to only a quarter of the section. In accordance with the theory, the lack of significant deformation caused by the sprays despite the high local pressures shows that the local peaks do not have a great importance in the response of the structure. The sprays created during the slamming and the extremely high water velocity along the body creates high stresses concentrations, see Figure 6.6, but no significant deformation. Moreover, the rapid decay in stress on the areas impacted previously highlight the importance of the dynamic pressure in the the slamming phenomenon. The hydrostatic force, although having a magnitude of 1 MPa, does not create any significant stress on the structure and is not the cause of the deformation. From this, one can deduce that the slamming impact is the only defining moment of the impact between a breaking wave and a platform column.

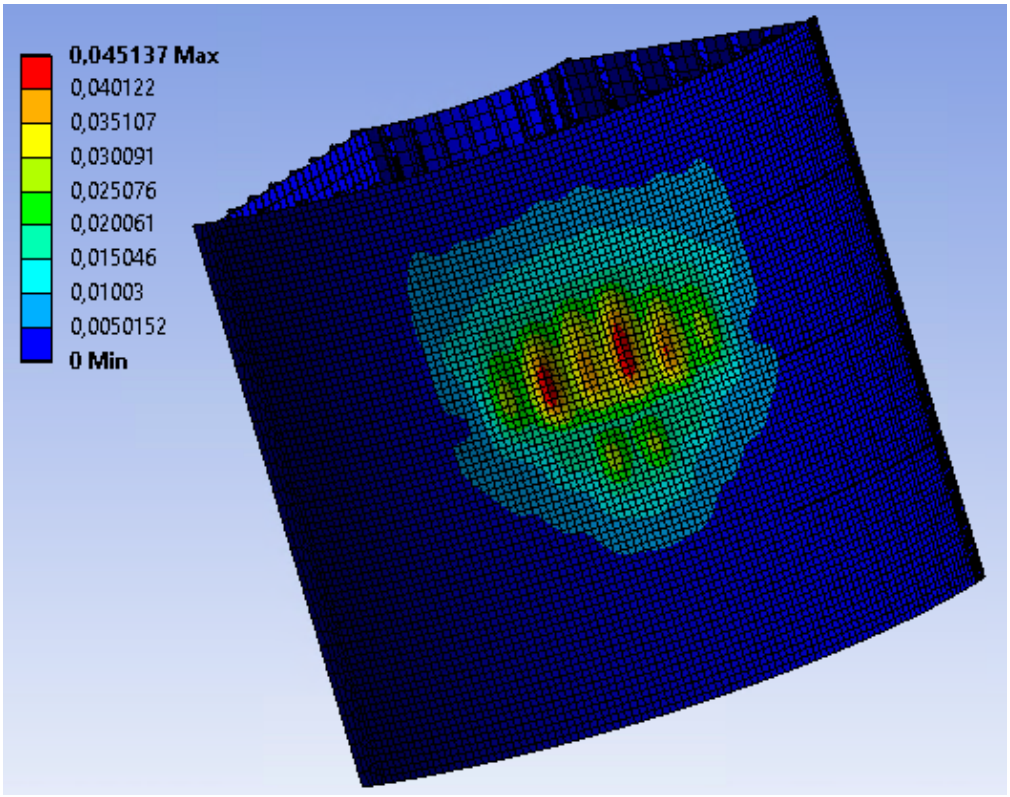

(a) Deformation of the outer panel

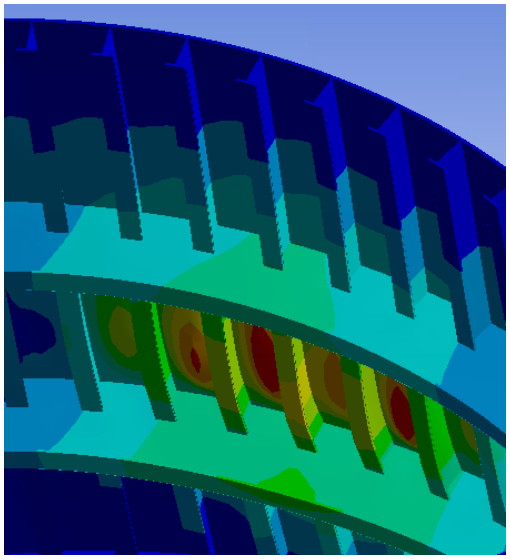

(b) Deformation of supporting members

Figure 6.3: Contour deformation on the column 20ms after impact. A maximum lateral deflection of 45mm is reached on the panel

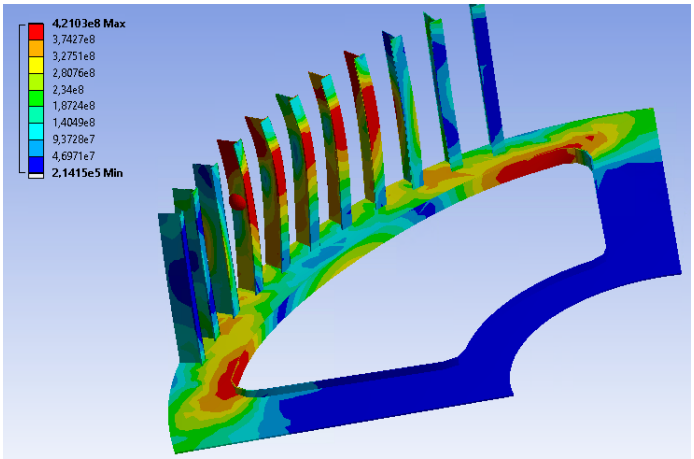

Figure 6.4: Stress contour on the internal structural members

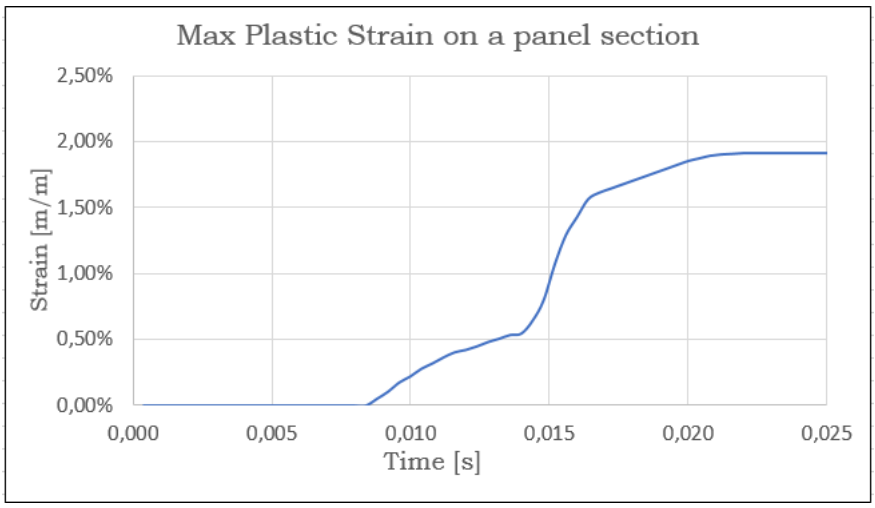

Figure 6.5: Graph of the maximum plastic strain on a section of the panel over time

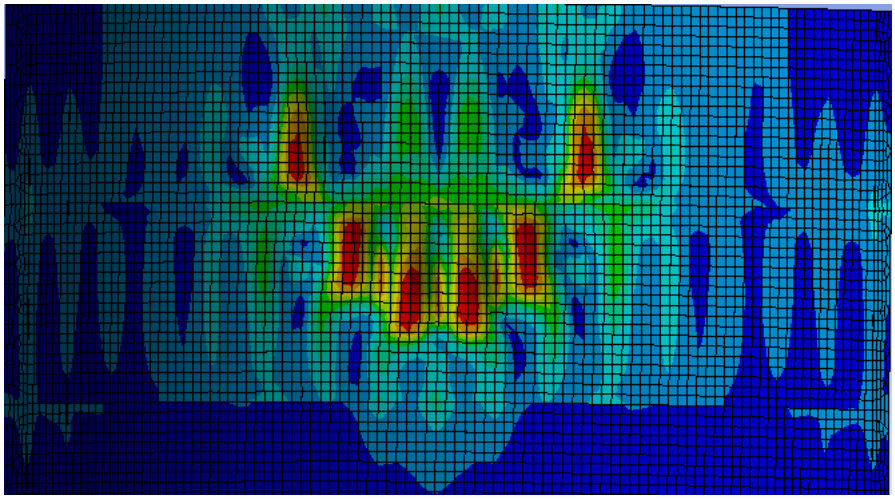

Figure 6.6: Stress concentration at the location of high dynamic pressures on the sides of the column do not cause permanent deformations

Chapter 7

Discussion

The results obtained in this study show the importance of elasticity in the slamming phenomenon and can raise questions as to whether model tests in basin are a relevant experiment in the slamming pressure investigation. A certain amount of parameters cannot be simulated at a small scale, such as compressibility, significant air cushions, plastic deformations, etc. The results are therefore flawed, and can lead to inaccurate guidelines for the design rules of marine structures.

One of the main parameters used for the assessment of damage on the structure used in this paper is straining. Real life materials are not ideal and can have defects or small cracks which can make fracture more likely but cannot be represented in such an analysis. Moreover, validated models for prediction of fracture both within a member and at joints between members are not available, so conservative assumptions had to be used. However, it was shown that strain-rate was important, especially with the moderately high rates obtained in this study. The maximal strain obtained for the two-way coupled analysis of the stiffened panel was 20% in about 15ms, which gives a strain rates with an order of magnitude of $10^1 s^{-1}$. Boyce and Dilmore (2009) carried out tensile tests and showed that high-strength steels displayed a yield stress more than 10% higher than the quasi-static yield stress, leading to reduced strain.

The slamming phenomenon is an extremely rapid event that needs to be analyzed dynamically with a very fine time stepping $\Delta t = 0.1 ms$. This accuracy is necessary in order to catch the varying forces acting on the structure. The meshes for both the fluid and structural domains need

to be in accordance in order to get accurate results and good convergence. Unfortunately, this could only be achieved for simple stiffened panels but not for the worst case scenario of the real scale simulation which had to be modified.

The analysis of curved stiffened model has shown that using a rigid body for pressure measurements leads to pressure peaks almost twice as high than with a real elastic-plastic material. Using this procedure, members of the model displayed local strains with value around 40%, which is dangerously high as far as material integrity is concerned. It is safe to assume that carrying such an experiment with the integral column model would have led to extremely large residual deformations, resulting in a possible failure of supporting members. This is why it is a necessity to perform two-way coupled fluid-structure interaction in events with large loading and therefore high deformations. Hydroelasticity has a major impact on the response of the structure, reducing deformations up to 75% in certain cases, and its effect becomes more significant with increasing velocity impacts (Louarn and Manganelli, 2010). Although deformations are still high in the area with a small deadrise angle, the column does not display any residual deformation where the deadrise is larger. The recommendation from DNV to consider a section of 45° for the structural analysis is therefore conservative, as a section of only 30° was found to be affected. The extent of the area subjected to large deformation is relatively small. This is due to the rapid decrease in the pressure coefficient with the increase in deadrise angle.

The choice of the the column shape is of great importance in the study of the slamming event. Semisubmersible platforms can offer different designs, with up to 8 structural columns. Both circular- and rectangular-shaped columns are used, and both designs offer particular interactions with breaking waves. One advantage of using a circular columns for the simulation is that the wave orientation does not matter as much as for rectangular columns. In this simulation, the impact was directed so that the point of lowest deadrise angle was located at the weakest point of the structure, so any other impact orientation would certainly give a smaller structural response. Using a deadrise angle of 7.5% for the full scale simulation, it is a certitude that the structure is able to withstand the slamming loads due to an extreme breaking wave. The damages are limited and acceptable for a rare event. However, Table 7.1 shows how the pressure

coefficient decreases with an increasing deadrise angle, and highlights the uncertainties linked with the results because they depend highly on the inclination of the column. Although the peak pressure is not a satisfying measure to determine the response, it is likely that the damages on the platform would be more significant with a less inclined column as the results from the analysis of stiffened panel show that an impact with a zero deadrise angle can cause strains an order of magnitude higher than those found on the full model.

Table 7.1: Maximum pressure coefficient C_p for various wedge deadrise angles (Johannessen, 2012)

α [deg]	$C_{p_{max}}$
4	546.3
7.5	137.
10	34.8
20	18.8
25	11

7.1 Limitations

As a first approach, it was agreed with Professor Amdahl that this study would be using the coupling component of Ansys in order to carry out the simulations, with the aim of testing the feasibility with this software suit, as a "bench-marking" work. Ansys Fluent has not seen any use at the Department of Marine Technology and as a result, nobody was able to provide guidance about the CFD solver Fluent, which lead to a long time spent to use Fluent properly both isolated and coupled with Ansys Mechanical. The original model used for the computation was slightly more complex but troubles in the convergence of the calculations and limitation in the computing speed of the simulation lead to a simpler model. The results are therefore non complete since the comparison between different inclinations of the column could not be made.

The principal limitation concerning the practical use of this work is the modeling of the wave. The complexity of nonlinear waves is very high and the proper modeling of a breaking-wave profile constitutes an actual in-depth study but a sensivity study could be carried out with varying overturning moment for the wave and thus different angles of impact on the structure.

Chapter 8

Conclusion and Recommendations for Further Work

8.1 Conclusion

An analysis of the impact of a breaking wave on an offshore platform column has been carried out in this Master's Thesis. The slamming event is challenging to depict accurately, as it requires large computational power and a precise configuration of the problem, but also due to the uncertainties inherent to the problem formulation. It leads to highly varying forces on structures and potentially hazardous damages to structures.

Using metocean data, a design wave was defined so that the impact between the fluid and the structure simulates a breaking wave with a return period of 10,000 years impacting the column of a semi-submersible platform. The simulation uses the coupling of a structural solver and a CFD solver in order to catch the impact of physical parameters such as hydroelasticity, which cannot be accounted for with experiments in basin with models. As a first approach, simple models of stiffened plates were used and two types of coupling were carried out in order to obtain a solution close to the real event. The two-way coupling displayed important results with regards to the estimation of slamming loads on marine structures. Hydroelasticity plays an important role during the slamming phenomenon, as it reduces greatly the fluid pressure on the structure as well as spreads the impact over a longer time than what it would be with a rigid

structure. The optimal method to analyze the fluid-structure interaction is therefore to use a numerical method by coupling computational fluid dynamics and structural analysis, as it reduces the lead time and the cost, for better relevance than test models. The results obtained with the two-way coupled analysis give large reductions concerning deformations and strains compared to the one-way coupling. The guidelines used in the industry might therefore be over-conservative. An analysis of a platform column subjected to slamming has then be carried out to assess the extent of the damage that could be caused by extreme environmental conditions. A constant deadrise angle of 7.5° was used for the column impacting the water. Using nonlinear FEM, the column was found to be able to withstand the loading with acceptable deformations.

8.2 Recommendations for Further Work

First of all, the completion of the coupled analysis for a complex structure and high velocity impact should be investigated, as the partial results do no offer the full response of the structure in time. Then, referring to the work of Muren (2016), it might be relevant to perform model test on flexible model in order to compare numerical and experimental results. The importance of several parameters such as compressibility of water, presence of air entrapment or strain-rate may also be assessed.

It could be interesting to investigate the behavior of the platform in damaged condition, and evaluate the response of another large breaking wave event on the deformed structure. The residual deformation can possibly weaken the structure and the repetition of impact could be harmful. A low-cycle fatigue analysis can be suitable.

Further, it might be interesting to go deeper into the hydrodynamic parameters of the study, such as comparing a turbulent and a laminar flow, but also creating an actual breaking wave profile. The constant deadrise angle in this study is due to the inclination of the column, but the direction of the flow in a breaking wave is actually constantly varying.

Bibliography

Abdussamie, N., Amin, W., Ojeda, R., and Thomas, G. (2014). Vertical wave-in-deck loading and pressure distribution on fixed horizontal decks of offshore platforms. *24th International Ocean and Polar Engineering Conference*.

Ajayi, K., Nwaji, G., and Ojo, O. (2014). Numerical study of the properties of high energy gas flow through a microturbine in 3d cascade. *Journal of Emerging Trends in Engineering and Applied Sciences*, 5:88–94.

Arai, M. and Miyauchi, T. (1998). Numerical study of the impact of water on cylindrical shells, considering fluid–structure interactions. *Elsevier Applied Science*, page 59–68.

Banner, M. L. and Peirson, W. L. (2007). Wave breaking onset and strength for two-dimensional deep-water wave groups. *Journal of Fluid Mechanics*, 585:93–115.

Benra, F.-K., Dohmen, H. J., Pei, J., Schuster, S., and Wan, B. (2011). A comparison of one-way and two-way coupling methods for numerical analysis of fluid-structure interactions. *Journal of Applied Mathematics*, 2011:1208–1217.

Bereznitski, A. (2001). Slamming: The role of hydroelasticity. *International Shipbuilding Progress*, 48:333–351.

Bonmarin, P., Rochefort, R., and Bourguel, M. (1989). Surface wave profile measurement by image analysis. *Experiments in Fluids*, 7:17–24.

Boyce, B. and Dilmore, M. (2009). The dynamic tensile behavior of tough, ultrahigh-strength steels at strain-rates from 0.0002 s^{-1} to 200^{-1}. *International Journal of Impact Engineering*, 36:263–271.

Campana, E., Carcaterra, A., Ciappi, E., and Iafrati, A. (2000). Some insights into slamming forces: compressible and incompressible phases. *Journal of Mechanical Engineering Science*, 214:881–888.

DNV (2010). *Recommended Practice C205: Environmental conditions and environmental loads*. Det Norske Veritas AS.

DNV (2013). *Determination of Structural Capacity by Non-linear FE analysis Methods*. Det Norske Veritas AS.

Duncan, J. H. (1983). The breaking and non-breaking wave resistance of a two-dimensional hydrofoil. *Journal of Fluid Mechanics*, 126:507–520.

Engle, A. and Lewis, R. (2003). A comparison of hydrodynamic impacts prediction methods with two dimensional drop test data. *Marine Structures*, 16:175–182.

Faltinsen, O. (1999). Water entry of a wedge by hydroelastic orthotropic plate theory. *Journal of Ship Research*, 43.

Faltinsen, O. (2000). Hydroelastic slamming. *Journal of Marine Science and Technology*.

Faltinsen, O. and Chezhian, M. (2005). A generalized wagner method for three-dimensional slamming. *Journal of Ship Research*, 49:279–287.

Faltinsen, O. and Zhao, R. (1993). Water entry of two-dimensional bodies. *Journal of Fluid Mechanics*, pages 593–612.

Gurney, T. (1979). *Fatigue of Welded Structures*.

Haque, M. and Hashmi, M. (1984). Stress-strain properties of structural steel at strain rates of up to 10^5 per second at sub-zero, room and high temperatures. *Mechanics of Materials*, 3:245–256.

Hong, L., Amdahl, J., and Wang, G. (2009). A direct design procedure for fpso side structures against large impact loads. *Journal of Offshore Mechanics and Arctic Engineering*, 131.

Hooke, R. (1678). *De Potentia Restitutiva, Or of Spring, Explaining the Power of Springing Bodies*.

Huse, E. and Nedrelid, T. (1985). Hydrodynamic stability of semisubmersibles under extreme weather conditions. *17th Annual OFfshore Technology Conference*.

Johannessen, S. (2012). Use of cfd to study hydrodynamic loads on free-fall lifeboats in the impact phase. Master's thesis, NTNU.

Kjeldsen, S. and Myrhaug, D. (1979). Wave-wave interactions, current-wave interactions and resulting extreme waves and breaking waves. *11th Annual Offshore Technology Conference*.

Kleefsman, T., Fekken, G., Veldman, A., and Iwanowski, B. (2004). An improved volume-of-fluid method for wave impact problems. *ISOPE*.

Larsen, E. (2013). Impact loads on circular cylinders. Master's thesis, NTNU.

Lian, G. and Haver, S. K. (2015). Measured crest height distribution compared to second order distribution. *14th International Workshop on Wave Hindcasting and Forecasting*.

Liu, T., Xie, W., and Khoo, B. (2008). The modified ghost fluid method for coupling of fluid and structure constituted with hydro-elasto-plastic equation of state. *Society for Industrial and Applied Mathematics*, 30:1105–1130.

Louarn, F. and Manganelli, P. (2010). A simplified slamming analysis model for curved composite panels. *21st International HISWA Symposium*.

Marcer, R., Berhault, C., de Jouëtte, C., Moirod, N., and Shen, L. (2010). Validation of cfd codes for slamming. *V European Conference on Computational Fluid Dynamics*.

Melville, W. K. and Matusov, P. (2002). Distribution of breaking waves at the ocean surface. *Nature*, 417:58–63.

Morison, J., Johnson, J., and Schaaf, S. (1950). The froce exerted by surface waves on piles. *Journal of Petroleum Technology*, 2:149–154.

Muren, M. (2016). Response calculations of semi-submersible column exposed to slamming loads. Master's thesis, NTNU.

Nedrelid, T. (1983). Future stability criteria for vessel survival tests of vessels in critical wave situations.

NORSOK (1994). *M-CR-120, Material Data Sheets for Structural Steel*. NORSOK.

NORSOK (2007). *NORSOK STANDARD N-003: Actions and action effects*. Norsok Standard.

Perlin, M., Choi, W., and Tian, Z. (2013). Breaking waves in deep and intermediate waters. *Annual Review of Fluid Mechanics*, 45:115–145.

Portemont, G., Deletombe, E., and Drazetic, P. (2004). Assessment of basic experimental impact simulations for coupled fluid/structure interactions modeling. *Journal of Crashworthiness*, 9:333–339.

Ramberg, W. and Osgood, W. R. (1943). Description of stress-strain cruves by three parameters. *National Advisory Committee for Aeronautics*.

Sandvik, K. (2004). Offshore structures – a new challenge. *XIV National Conference on Structural Engineering*.

Stansell, P. and MacFarlane, C. (2002). Experimental investifation of wave breaking criteria based on wave phase speed. *Journal of Physical Oceanography*, 32:1269–1283.

Stokes, G. (1880). *Appendices and supplement to a paper on the theory of oscillatory waves*. Math. Phys. Pap.

Storheim, M. and Amdahl, J. (2015). On the sensitivity to work hardening and strain-rate effects in nonlinear fem analysis of ship collisions. *Ships and Offshore Structures*.

Thomas, G., Davis, M., Holloway, D., and Roberts, T. (2006). The effect of slamming and whipping on the fatigue life of a high-speed catamaran. *Journal of Mechanical Engineering*, 3:165–174.

Tian, Z., Perlin, M., and Choi, W. (2010). Energy dissipation in two-dimensional unsteady plunging breakers and an eddy viscosity model. *Journal of Fluid Mechanics*, 655:217–257.

von Karman, T. (1929). The impact on seaplane floats during landing. *National Advisory Committee for Aeronautics*.

Voogt, A. and Soles, J. (2007). Stability of deepwater drilling semi submersibles. *10th International Symposium on Practical Design of Ships and Other Floating Structures*.

Voogt, A., Soles, J., and Dijk, R. (2002). Mean and low frequency roll for semi-submersibles in waves. *12th International Offshore and Polar Engineering Conference*, pages 379–384.

Wagner, H. (1932). Über stoß- und gleitvorgänge an der oberfläche von flüssigkeiten. *Zeitschrift für Angewandte Mathematik und Mechanik*.

Wang, G., Basu, R., Chavda, D., and Liu, S. (2005). Rationalizing the design of ice strengthened side structures. *ABS Technical Papers*.

Wang, G., Tang, S., and Shin, Y. (2002). A direct calculation approach for designing a ship-shaped fpso's bow. *12th International Offshore and Polar Engineering Conference*.

Wienke, J. and Oumeraci, H. (2005). Breaking wave impact force on a vertical and inclined slender pile - theoretical and large-scale model investigations. *Coastal Engineering*.

Wienke, J., Sparboom, U., and Oumeraci, H. (2004). Theoretical formulae for wave slamming loads on slender circular cylinders and application for support structures of wind turbines. *International Conference on Coastal Engineering*.

Zhao, R., Faltinsen, O., and Aarsnes, J. (1996). Water entry of arbitrary two-dimensional sections with and without flow separation. *21st Symposium on Naval Hydrodynamics*, pages 408–423.

Zienkiewicz, O., Taylor, R., and Zhu, J. (2005). *Finite Element Method, Its Basis and Fundamentals*. Det Norske Veritas AS, 6th edition.